José María Carmona Pérez

De:	eesserver@eesmail.elsevier.com en nombre de José Cruz <eesserver@eesmail.elsevier.com>
Enviado el:	dimarts, 19 / de novembre / 2019 21:49
Para:	José María Carmona Pérez; jmcarmonabcn@gmail.com
CC:	bparker@uoguelph.ca; Jofre Herrero Ferran; Diana Puigserver Cuerda
Asunto:	Your Submission

Ms. Ref. No.: STOTEN-D-18-07872R2
Title: Natural attenuation of pools and plumes of carbon tetrachloride and chloroform in the transition zone to bottom aquitards and the microorganisms involved in their degradation
Journal: Science of the Total Environment

Dear Dr. Carmona,

I am pleased to inform you that your paper "Natural attenuation of pools and plumes of carbon tetrachloride and chloroform in the transition zone to bottom aquitards and the microorganisms involved in their degradation" has been accepted for publication in STOTEN and forwarded to the publishers.

Your accepted manuscript will now be transferred to our production department and work will begin on creation of the proof. If we need any additional information to create the proof, we will let you know. If not, you will be contacted again in the next few days with a request to approve the proof and to complete a number of online forms that are required for publication.

For any production related questions please contact Pallavi Das(Journal Manager) at j.scitotenv@elsevier.com. There is no need to contact the editors.

Thank you for giving us the opportunity to review your article.

Sincerely,

José Virgílio Cruz, Ph.D.
Associate Editor
Science of the Total Environment

Comments from the Editor:

Natural attenuation of pools and plumes of carbon tetrachloride and chloroform in the transition zone to bottom aquitards and the microorganisms involved in their degradation

***Graphical Abstract**

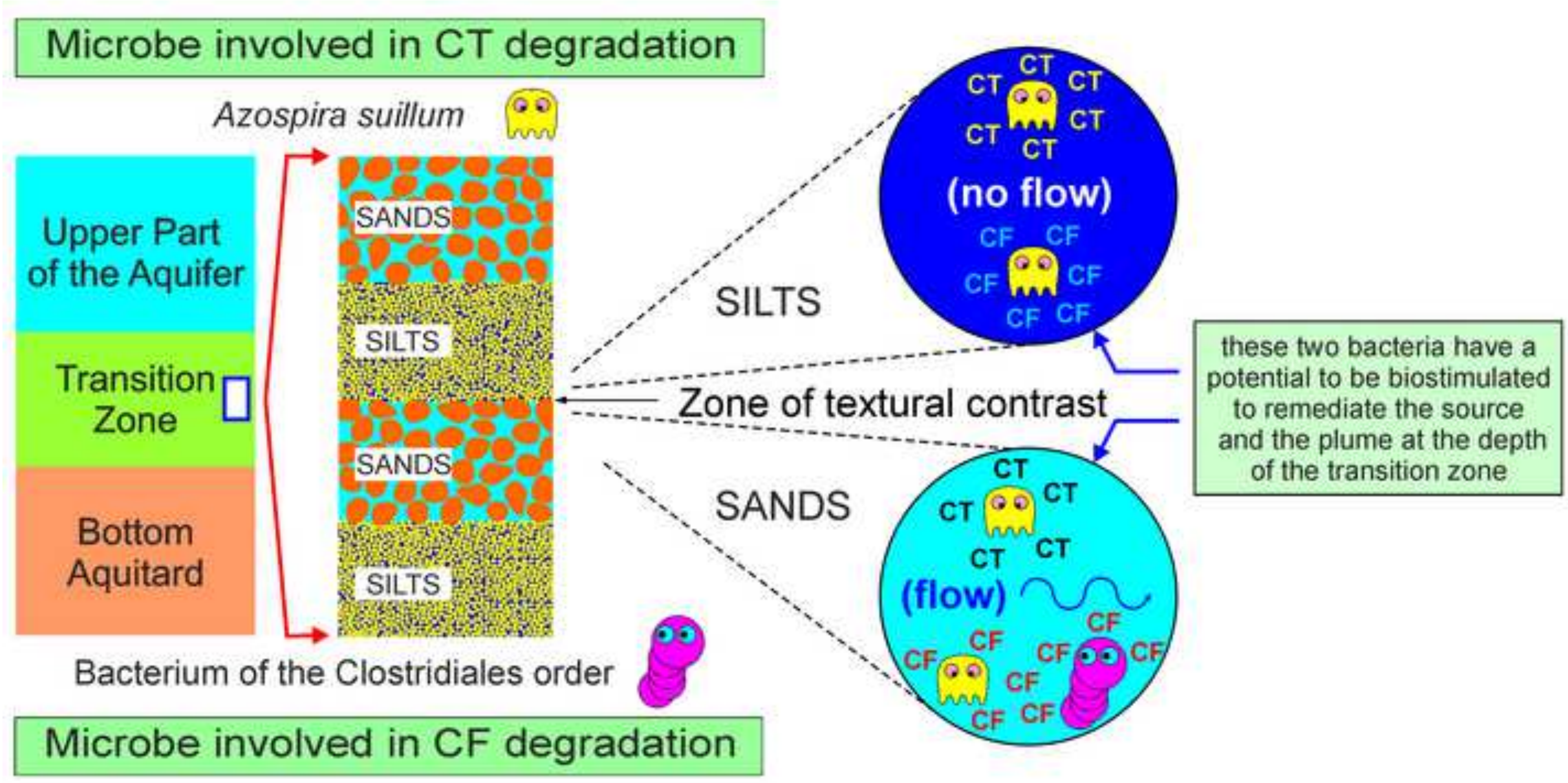

these two bacteria have a potential to be biostimulated to remediate the source and the plume at the depth of the transition zone

***Highlights (for review : 3 to 5 bullet points (maximum 85 characters including spaces per bullet point)**

- Pools of chlorinated solvents in the transition zone could be remediated
- Dominant redox conditions and isotope approaches allow to identify dechlorination
- Microorganisms involved in dechlorination were identified at field scale
- *Azospira suillum* led to a more effective dechlorination in the transition zone
- Biostimulation of these microorganisms could be a plausible remediation strategy

***conflict of Interest Statement**

Declaration of interests

☒ The authors declare that they have no known competing financial interests or personal relationships that could have appeared to influence the work reported in this paper.

☐The authors declare the following financial interests/personal relationships which may be considered as potential competing interests:

Natural attenuation of pools and plumes of carbon tetrachloride and chloroform in the transition zone to bottom aquitards and the microorganisms involved in their degradation

Diana Puigserver[a], Jofre Herrero[b], Beth L. Parker[c] and José M. Carmona[d*]

[a] Dept. of Mineralogy, Petrology and Applied Geology. Faculty of Earth Sciences. University of Barcelona. C/ Martí i Franquès, s/n. E-08028 Barcelona (Spain). puigserverdiana@ub.edu

[b] Dept. of Mineralogy, Petrology and Applied Geology. Faculty of Earth Sciences. University of Barcelona. C/ Martí i Franquès, s/n. E-08028 Barcelona (Spain). jofreherreroferran@ub.edu

[c] School of Engineering, University of Guelph 50, Stone Road East, Guelph, N1G 2W1 (Ontario, Canada). bparker@uoguelph.ca

[d] Dept. of Mineralogy, Petrology and Applied Geology. Faculty of Earth Sciences. University of Barcelona. C/ Martí i Franquès, s/n. E-08028 Barcelona (Spain). jmcarmona@ub.edu

* Corresponding author

Abstract

In the transition zone between aquifers and aquitards, DNAPL pools of carbon tetrachloride and chloroform accumulate because of heterogeneity in this zone. Natural attenuation occur at pools and plumes, indicating that remediation might be possible. The aims of the study were: i) to assess the role of heterogeneity in the natural attenuation of these compounds, ii) determine degradation processes within this zone, and iii) identify dechlorinating microorganisms. For this, groundwater concentrations, redox-sensitive parameters, CSIA isotopic and DGGE molecular techniques were used. The main findings at depth of the transition zone were: (1) The important key control played by heterogeneity on natural attenuation of contaminants. (2) Heterogeneity caused the highly anoxic environment and dominant sulfate-reducing conditions, which accounts for more efficient natural attenuation. (3) heterogeneity also explains that the transition zone constitutes an ecotone. (4) The bacteria size exclusion is governed by the pore throat threshold and determines the penetration of dechlorinating microorganisms into the finest sediments, which is relevant, since it implies the need to verify whether microorganisms proposed for bioremediation can penetrate these materials. (5) Reductive dechlorination caused the natural attenuation of contaminants in groundwater and porewater of fine sediments. In the case of carbon tetrachloride, it was an abiotic process biogenically mediated by A. suillum, a bacterium capable of penetrating the finest sediments. In the case of chloroform, it was a biotic process performed by a Clostridiales bacterium, which is unable to penetrate the finest materials. (6) Both microorganisms have potential to be biostimulated to dechlorinate contaminants in the source and the plume in the transition zone. These outcomes are particularly relevant given the longevity of DNAPL sources and have considerable environmental implications as many supply wells in industrial areas exploit aquifers contaminated by chlorinated solvents emerging from DNAPL pools accumulated on the low-conductivity layers in transition zones.

Keywords

geological and textural heterogeneity in the transition zone; carbon tetrachloride; chloroform; natural attenuation; reductive dechlorination; *Azospira suillum*

1. Introduction

Carbon tetrachloride (CT) and chloroform (CF) are chlorinated solvents that belong to the group of dense non-aqueous phase liquids (DNAPLs). Together with dichloromethane (DCM) and chloromethane (CM), they are known as chloromethanes. CT and CF have been widely used as precursors of refrigerants (Xiao et al., 2000), and are pollutants harmful to the ozone layer (Fraser et al., 2014), ecosystems, and human and animal health, as they are toxic and carcinogenic. As other chlorinated solvents, CT and CF DNAPLs and plumes are often found in industrial areas that have been subjected to strong anthropic pressure.

Chlorinated solvents can last in the environment from decades to hundreds of years as a result of: (1) their low solubility as a free or residual phase; (2) their low natural attenuation (NA) rates when redox conditions are not sufficiently anoxic; (3) the different phases in which they can be partitioned (Pankow and Cherry, 1996); and (4) the portion of them that penetrate through molecular diffusion into the porewater of fine sediments (PWFS), as described in Parker et al. (2004). They cause considerable pollution episodes in groundwater (Mackay and Cherry, 1989; Cohen and Mercer, 1993; Pankow and Cherry, 1996). Their distribution in the subsurface is quite complex due to geological heterogeneity, which determines not only their distribution as DNAPLs at the source but also the morphology of the emanating plume (Imhoff et al., 1994; Farthing et al., 2012). In the free phase, they migrate vertically through the most permeable formations, leaving a trail of immobile residual DNAPL that partially occupies the porosity at saturations below the residual saturation value in granular media (Hartog et al. 2010; ITRC, 2015; Fetter et al., 2017). This trail can be progressively dissolved and incorporated into the groundwater flow, while the free phase tends to accumulate as pools at different depths on layers of low hydraulic conductivity (Rivett et al., 2014) and at the bottom of the aquifer (Pankow and Cherry, 1996; Luciano et al., 2010; Fjordbøge et al., 2017; Einarson et al., 2018), occupying a large portion of pores (ITRC, 2015) and making hydraulic conductivity decrease at the source (Fetter et al., 2017).

This pattern is especially noteworthy in cases where a transition zone to a bottom aquitard exists in the lowermost part of an aquifer. In this zone, an intrinsically huge geological heterogeneity occurs because of the presence of numerous interstratified silty-clay levels between sands (Puigserver et al., 2013). This heterogeneity results in a great variability in hydraulic conductivity, and globally, in a whole low value of this parameter, which results in a low groundwater velocity and a minor supply of dissolved oxygen (DO). The low hydraulic conductivity reaches an even lower value because of the large percentage of porosity occupied by DNAPL when the source is in the transition zone. In this scenario, the subsequent lower velocity leads to a minor DO supply and to lesser groundwater flushing and dissolution rate at the source, which accounts for the greater longevity of sources and plumes in transition zones compared with other more conductive depths in the aquifer (Puigserver et al., 2016a, b). The accumulation of DNAPL pools in the transition zone has significant environmental implications as many supply wells in the world exploit aquifers that, from the geological point of view, constitute deposits whose lower parts are transition zones.

Cases have been described in which the high concentrations of CT and CF in the source can harm or partly inhibit microbial dechlorinating activity (Da Lima, and Sleep, 2010). However, these pollutants, like other chlorinated solvents, can be degraded naturally by biotic and abiotic reductive dechlorination under appropriate redox anoxic conditions (Ramsburg et al., 2010) in the source and the plume (Hunkeler et al., 2011; Wanner et. al, 2016). Davis et al. (2003) reported the reductive abiotic dechlorination of CT to form CF in the presence of iron-reduced minerals. Penny et al. (2015) observed that only a minor portion of bacteria from anoxic media were capable of degrading CT in the laboratory. Puigserver et al. (2016c) identified *Azospira suillum* (formerly *Dechlorosoma suillum*, Achenbach et al., 2001) in microcosm experiments at laboratory scale with real field samples from the same site as this work and noted the unique presence of this microorganism (and another belonging to the order Clostridiales) when redox conditions became sulfate-reducing and the abiotic reductive dechlorination of CT to CF occurred. These examples corroborate that the assessment of the dominant redox conditions in sources and plumes is crucial to understanding the fate of these pollutants and to evaluate remediation strategies. In the case of the transition zone, the examples suggest that the minor supply of DO and the subsequent occurrence of anoxic conditions favor in situ biotic or abiotic remediation of the source and the plume.

Christensen et al. (2000), in a review on the characterization of the dominant redox conditions in groundwater contaminant plumes, demonstrated that these conditions, which control the biotic and abiotic processes occurring in the environment, could be evaluated according to the relative distribution of contaminants with respect to the redox-sensitive inorganic species together with other parameters and approaches such as redox potential (Eh), total organic carbon (TOC), and use of the Compound-Specific Isotope Analysis technique (CSIA).

The aims of the current study were: i) to assess the role played by geological and textural heterogeneity in the transition zone in the degradation of CT and CF, ii) to determine the degradation processes of these compounds in this zone and evaluate the magnitude of NA processes, and iii) to identify the microorganisms involved in the NA of these compounds. To this end, a site was chosen for the current study where an unconfined aquifer was affected by CT and CF contamination.

2. Site description

The study site is located in the La Pineda petrochemical complex (Tarragona, Spain, 100 km south of Barcelona), which became active in stages, beginning in 1960. Two main pollutants caused contamination by CT and CF in an unconfined granular aquifer. The pollution was detected in 1996 in one of the plants of the complex, although it is unknown when the contamination first appeared. These compounds were used in refrigerant production (Puigserver et al., 2013) and were stored independently in two tanks. Spillages, which occurred repeatedly, varied in duration and accumulated on the numerous layers of low hydraulic conductivity in the transition zone and on the geologic contact with the bottom aquitard. In addition, superimposed upon this contamination, other contamination episodes occurred in the past, resulting in a complex pattern of contamination characterized by a variety of compounds from different origins (other chloromethanes, chloroethenes, chloroethanes, BTEX, PAHs and metals). Furthermore, agricultural land uses upgradient of the petrochemical complex give rise to groundwater pollution by inorganic co-contaminants, nitrates, and sulfates related to fertilization practices. These electron acceptors migrate with groundwater flow and reach the industrial area, where the contamination by CT and CF exists.

A substantial portion of the pollutants penetrated via molecular diffusion into the PWFS (Puigserver et al., 2013). Despite the considerable decrease in the concentrations of

CT and CF in groundwater between 1997 and 2009 (maximum values in 1997 of 771 and 19,370 μg/L for CT and CF, respectively; and in 2009, of 308.2 and 552.1 μg/L, respectively), pollution continued to be above the parametric values due to the application of the pump-and-treat remediation system, which reached its limit of effectiveness (Puigserver et al., 2016a).

The groundwater monitoring network (Figure 1) consists of 26 conventional piezometers and two multilevel wells (CMT 7 ports, Solinst). Conventional piezometers (with depths ranging from 11 to 20 m, Figure 2A) consist of: 1) a first section of blind pipe (i.e., non-screened) reaching depths ranging from 10 to 12 m; 2) a second section of screened pipe that is open from the upper part of the aquifer (UPA) to its lower part, which is a transition zone to a bottom aquitard (TZBA)(see Section 4.1); and 3) a third short section of blind pipe for piezometers deeper than 17 m (depth where a clayey bottom aquitard exists). The two multilevel wells (S1UB and S2UB) are 220 m downstream of the source and are located 5 m apart (Figure 1). Port 7, the deepest of the seven ports of S1UB and S2UB, are 12.60 and 12.80 m deep, respectively. To construct these multilevel wells, boreholes B-S1UB and B-S2UB were drilled (22.00 and 16.37 m deep, respectively) and equipped as multilevel wells. The analysis of the stratigraphic logs of the monitoring network allowed determination of the lithological and textural characteristics of the subsoil in the site area. Moreover, emplacement of the monitoring network allowed the study of variations in groundwater quality.
According to the historical evolution of the concentrations of CT and CF along the flow path, there are two sources, including the main source (from conventional piezometer S5-P2 to P7) and a smaller, secondary source detected immediately upstream from P8 (Figure 1 and Figure 2A).

3. Materials and methods

The methodological procedures shown in this section were followed to attain the objectives raised in the study (see Section 1). These procedures allow the assessment of the role of geological and textural heterogeneity in the transition zone in degradation of CT and CF. To define that role, the determination of the dominant redox conditions and the identification of the biogeochemical processes occurring under these conditions were carried out. This was done along the flow and with depth comparing the results in the UPA (a very homogeneous hydrostratigraphic unit) with the TZBA (an extremely heterogeneous unit). For this, the groundwater sampling to analyze redox-sensitive species allowed: i) identifying the dominant redox conditions, ii) verifying if NA of CT and CF was occurring, and iii) if NA was more efficient in the TZBA. The determination of the NA rate of these compounds (λ) and the isotopic enrichment factor (ε) allowed quantifying the magnitude of this degradation. The results acquired from the bacterial community analysis, permitted: i) the identification pf the hydrostratigraphic unit where microbial diversity and abundance were greater, and ii) identifying which were the microorganisms involved in degradation of CT and CF. The integration of these results with the previous referring to the biogeochemical processes and redox conditions in which these processes occurred, allowed determining in which hydrostratigraphic unit the dechlorinating microorganisms were more efficient and under what redox conditions they achieved this task.

3.1 Dominant redox conditions and degradation processes

To assess the dominant redox conditions in the subsurface of the studied site, the guidelines established by Christensen et al. (2000) and subsequently implemented by many other authors (Rotiroti et al., 2018; Weatherill et al., 2018) were followed in the current work. They consist in characterizing the dominant redox processes in groundwater, which allowed identification of the dominant redox conditions under which these processes occurred. These dominant redox conditions determine the redox zone to which the environment is assigned. These redox zones refer to the classical model that, from the thermodynamic point of view, establishes a vertical sequence of the dominant electron acceptors in natural water and sediment systems. In this model, in descending potential of metabolic energy yield, oxygen, nitrate/nitrite, Mn^{4+}/Mn^{2+}, Fe^{3+}/Fe^{2+}, sulfate/sulfide, and CO_2/CH_4 are the successive oxidizing agents with increasing depth (i.e., with a gradient in redox conditions that varies from completely oxidizing to extremely reducing).

Analyses of groundwater samples in conventional piezometers and multilevel wells in the monitoring network allowed the study of the variability of groundwater quality and to determine the dominant redox conditions and degradation processes along the flow path in the transition zone and with depth, respectively. Samples taken in conventional piezometers represent all flow lines crossing the section of screened pipe in the influence area of the sampling pump at the depth to which it is placed. Analytical results are therefore, an integrated value of the mentioned flow lines. In contrast, groundwater taken in the sampling ports (4 cm long) of multilevel wells allowed obtaining greater accuracy in the representation of results with depth. The following parameters and concentrations were determined along the flow path and with depth: (1) temperature, electrical conductivity and pH, which were measured on site when sampling; (2) Eh and DO, which were recorded on site, as well as other redox-sensitive parameters (TOC, nitrate, nitrite, Mn^{2+}, Fe^{2+}, and sulfate, which were analyzed in the laboratory); and (3) chloromethanes.

In addition, the CSIA technique was applied to the groundwater samples from the same piezometers and wells as a tool to study and characterize the degradation processes of CT and CF (US EPA, 2008) by determining their isotopic fractionation ($\delta^{13}C$ values). The CSIA technique is a powerful tool in the characterization of the degradation processes of chlorinated solvents (US EPA, 2008). In general, the degradation of a compound more easily affects molecules with light isotopes, resulting in a relative enrichment in molecules with heavy isotopes in the groundwater (^{12}C and ^{13}C, respectively in the case of CT and CF). Furthermore, $\delta^{15}N$ and $\delta^{18}O$ values of nitrate, and $\delta^{34}S$ and $\delta^{18}O$ of sulfate were also used to identify denitrifying and sulfate-reducing processes (the reduction potential of these inorganic compounds is greater than that of CT and CF, and therefore the degradation of the last two compounds is partially inhibited).

The λ and ε values to evaluate the extent of degradation of CT between two conventional wells A and B separated from each other by a distance d (in meters) were calculated along the flow path in the source area and along the centerline of the plume. The equation $\lambda = \ln(f)/d$ (Hunkeler et al., 2008) was used to calculate the rate of attenuation (λ, in m^{-1}). In this equation, f is the remaining fraction of the contaminant in well B (located downgradient from well A), therefore, $f = C_B / C_A$, where C_A is the concentration in well A and C_B is the concentration in well B. In turn, the isotope enrichment in ^{3}C (ε, in ‰) was calculated using the following equation: $\varepsilon = (\alpha - 1)\cdot 1000$ (Hunkeler et al., 2008), where $\alpha = (1000 + \delta^{13}C_A)/(1000 + \delta^{13}C_B)$ is the isotope fractionation factor of ^{3}C, in which subscripts A and B refer to wells A and B, and $\delta^{13}C$ refers to CT. These two equations were also used to analyze the rate of attenuation and the enrichment factor of CT with depth in the two multilevel wells in the plume. In this case, the maximum concentration at the source (in conventional piezometer P7, Figure 4A.C) was taken as C_A, whereas C_B in the UPA and TZBA (Figure 2A) were the average concentrations in the sampling ports of the multilevel wells (1, 3 and 4 for the UPA and 5, 6 and 7 for the TZBA). The values of λ and ε for the case of CF were also calculated using the previous equations (with $\delta^{13}C$ referred to CF).

The λ and ε values of nitrate and sulfate between two conventional wells were also calculated along the flow path in the source area and along the centerline of the plume, as well as from the source area to the sampling ports of multilevel wells in the UPA and TZBA. In all these cases, the background concentration of these co-contaminants in the zone upgradient of the main source of CT and CF were taken as C_A. The $\delta^{15}N$ and $\delta^{34}S$ values were used to calculate the ε value of nitrate and sulfate, respectively.

3.1.1 Sampling protocols and procedures

Conventional piezometers in the monitoring network that approximately followed a profile along the centerline of the source and plume (Figure 1 and Figure 2A) were used to sample groundwater from the TZBA. In these piezometers, groundwater was pumped from the depth of the contact TZBA-BA (similar to that of port 7, the deepest of multilevel wells). Multilevel wells S1UB and S2UB were used to sample groundwater with depth in the plume (ports 1 to 4 at the UPA, and ports 5 to 7 at the TZBA). In addition, groundwater and fine sediments were sampled in wells and boreholes to determine dissolved TOC contents and particulate organic matter, respectively, upgradient of the petrochemical complex at the depth of the TZBA. Groundwater samples were taken using an Eijkelkamp peristaltic pump and an Integra Solinst Bladder pump (Georgetown, Ontario, Canada) depending on the depth of the piezometers and multilevel wells. A flow cell (Solinst) was used to ensure intact redox conditions during the purging and sampling operations and when measuring physicochemical parameters on site. Aqueous samples were collected in 100-mL VOC glass serum bottles (Supelco Analytical) for concentration analyses and in 120-mL amber screw-cap bottles (Supelco Analytical) for carbon isotope analyses. Sodium azide (N_3Na; Fluka, Tres Cantos-Madrid, Spain) was added to the groundwater samples immediately upon collection to inhibit bacterial activity following procedures reported by Trevors (1996). For TOC concentrations, 120-mL amber screw-cap bottles (Supelco Analytical) were used (analytical quality hydrochloric acid, Merck, was used to acidulate these samples up to a pH of 3). The groundwater samples for nitrate and sulfate analyses were collected in 150-mL translucent plastic bottles, and Pyrex glass bottles were used for $\delta^{15}N_{nitrate}$, $\delta^{18}O_{nitrate}$, $\delta^{34}S_{sulfate}$, and $\delta^{18}O_{sulfate}$ analyses. Groundwater samples for Mn and Fe were collected in 14-mL transparent plastic vials. The samples were conserved at 4 °C. The sampling and conservation protocols indicated in Puls and Barcelona (1996) and Johnston (2006) were used during transport and at the laboratory. The field blanks that were taken (blanks of instrumentation, conservation reagents, and transportation to laboratory) are indicated, among other aspects, in these protocols. In addition to these blanks, each sample of groundwater was taken in duplicate to have a good control of the analytical results in the laboratory.

PWFS is water fundamentally immobile and enclosed inside the tiny pores of fine sediments of the formation (silty sands, silts and clays, and clayey and silty matrices of coarse sediment). PWFS and the corresponding fine sediment fraction were sampled at different depths from boreholes B-S1UB and B-S2UB (drilling procedures and core recovering protocols are described in Puigserver et al., 2013). The purpose of these samples was to analyze the diversity and abundance of microbial communities and to identify the microorganisms involved in CT and CF degradation in the PWFS.

3.1.2 Laboratory analytical methods, techniques and instrumentation

The samples were analyzed at laboratories of the Scientific and Technological Centers of Barcelona University. These laboratories implement a quality management system based on the ISO 9001:2015 standard. This implies that a strict laboratory control sampling protocol was followed, which included the use of laboratory blanks and standard reference materials.

As a quality control of the laboratory analytical results, the absolute relative percent difference (RPD%) calculation between the field duplicates was used as a measure for evaluation of the precision of these results. For this calculation, the absolute value of the difference between the analytical results of the two duplicates is divided by the absolute value of the average of the two results. The value obtained is expressed as a percentage multiplying it by 100:

$$\mathrm{RPD\%} = [|D1 - D2| / ((|D1 + D2|) / 2)] \times 100$$

where $|D1 - D2|$ and $|D1 + D2|$ are the absolute values of the difference and summation of the duplicate sample results, respectively.

The RPD% values for CT concentrations between 1.7 and 0.2 µmol/L varied from 4.57 to 13.03%, respectively; and for concentrations between 0.2 and 0.014 µmol/L, it varied from 13.03% to 15.48%. In the case of CF, the RPD% values for concentrations between 10.7 and 0.3 µmol/L varied from 2.67 to 4.77%, respectively; and for concentrations between 0.3and 0.02 µmol/L varied from 4.77 to 15.01%. For DCM between 0.3and 0.042 µmol/L varied from 4.69 to 11.98%, respectively; and between 0.042 and 0.021 µmol/L varied from 11.98 to 13.10%. For CM between 1.0 and 0.13 µmol/L varied from 6.35 to 12.27%, respectively; and between 0.13and 0.033 µmol/L varied from 12.27 to 15.74%.

As regards the ^{13}C isotopic composition of chloromethanes, only the RPD% values for CT and CF were calculated, given the very low concentrations of DCM and CM. The $\delta^{13}C_{CT}$ maximum, average, and minimum RPD% values, were 1.41, 0.92, and 0.28%, respectively. In the case of $\delta^{13}C_{CF}$, those values were 1.29, 0.91, and 0.27%, respectively.

The RPD% values for $\delta^{15}N_{Nitrate}$ and $\delta^{18}O_{Nitrate}$, and for $\delta^{34}S_{Sulfate}$ and $\delta^{18}O_{Sulfate,}$ were also calculated. The $\delta^{15}N_{Nitrate}$ maximum, average, and minimum RPD% values were 2.63, 1.20, and 0.56%, respectively; and for $\delta^{18}O_{Nitrate}$, they were 7.50, 2.83, and 0.45%, respectively. The $\delta^{34}S_{Sulfate}$ maximum, average, and minimum RPD% values were 4.59, 1.78, and 0.52%, respectively; and for $\delta^{18}O_{Sulfate}$, they were 5.01, 2.38, and 0.56%, respectively.

The chloromethanes concentrations were measured using gas chromatography-mass spectrometry (GC-MS). The limits of quantification (LOQ), as a measure of sensitivity of results, were (in µmol/L): 0.0075 (CT), 0.0159 (CF), 0.0171 (DCM), and 0.0297 (CM).

A protocol based on the extraction of VOCs by direct adsorption from the aqueous phase was used to determine the δ^{13}C of chloromethanes. The extraction was conducted by inserting an adsorbent fiber (SPME fiber assembly 75 mm carboxen/polydimethylsiloxane (PDMS), Supelco (Madrid, Spain)) into the water sample, which was stored in a 100-mL amber glass bottle (Supelco Analytical) and closed with a silicone septum and agitated for 30 min to adsorb the chloromethanes. The determination of $\delta^{13}C$ was performed using gas chromatography-combustion isotope ratio mass spectrometry (GC-CIRMS) following the protocol described in Palau et al. (2007) and using a Delta C Finnigan (an earlier name of Thermo Fisher Scientific, Inc.) MAT IRMS spectrometer (Thermo Fisher Scientific Inc., Waltham, MA, USA). TOC was analyzed using a TOC-5000 TOC analyzer (Shimadzu). The sulfate, nitrate, and nitrite concentrations were analyzed following the EPA 9056 protocol using ion chromatography. The pretreatment protocols used to determine the nitrate and sulfate isotopic compositions were those indicated in Dogramaci et al. (2001) for determining $\delta^{34}S_{sulfate}$ and $\delta^{18}O_{sulfate}$, and in Silva et al. (2000) and Fukada et al. (2003) for obtaining $\delta^{15}N_{nitrate}$ and $\delta^{18}O_{nitrate}$. The resulting precipitates were analyzed using isotope ratio mass spectrometry (IRMS).

3.2 Bacterial community analysis

To assess the diversity and abundance of microorganisms with depth, in the case of biotic degradation, denaturing gradient gel electrophoresis (DGGE) analyses were conducted in the groundwater samples obtained from ports of the multilevel wells S1UB and S2UB and in the samples of PWFS from fine sediment cores recovered from boreholes B-S1UB and B-S2UB.This technique involves the separation pattern of polymerase chain reaction (PCR)-amplified 16S rDNA gene fragments in polyacrylamide gels with a linearly increasing gradient of denaturants (Muyzer et al., 1993). The number of DGGE bands corresponds to the number of main members in the microbial community. Although ideally, one band on the gel corresponds to one species (Cycoń et al., 2013), and hence, the number of bands is an indicator of the sample’s diversity. The relative abundance of a microorganism can be estimated by measuring the brightness intensity of its bands relative to the intensity of all the bands in the analyzed samples.

The sampling protocols and procedures used to obtain fine sediments from the cores of the boreholes B-S1UB and B-S2UB are described in Puigserver et al. (2013). DGGE electrophoresis of PCR-amplified 16S rRNA genes was run in denaturing acrylamide gels and stained prior to photography following standard methodologies. Unweighted DGGE band data were used to assess the diversity in each groundwater and PWFS sample, i.e., the presence or absence of DGGE bands in each lane sample. Weighted data were used to evaluate the abundance of a microbial community in a lane sample considering the brightness intensity of each band relative to the intensity of bands in all the analyzed samples, including the lanes of two DGGE band markers, denoted as operational taxonomic unit 6 (OTU 6) and 15 (OTU 15) in the current work. These two OTUs correspond to the two microorganisms that Puigserver et al. (2016c) found to be involved in CT and CF degradation (*A. suillum* and a Clostridiales bacterium, respectively, see Section 1).

To identify the presence of these microorganisms at the field scale (i.e. with depth in groundwater from multilevel wells S1UB and S2UB, and in PWFS from boreholes B-S1UB and B-S2UB), results of DGGE analyses were combined with those obtained in a clone library analysis. Detailed information on the microbiological and clone library analysis is described in the Supplementary Data (SD).

4. Results and discussion

4.1 Geological and hydrogeological framework

The aquifer is composed of Quaternary prograding alluvial fan deposits, at the base of which, there is a transition zone that corresponds to sheet flood deposits associated with the alluvial fans. Groundwater flows towards the Mediterranean Sea, according to the slight dip of the subsoil layers (Figure **2**A) to the southeast. The water table oscillates between 5.5 and 9 m below ground level, with an average maximum water table oscillation of 1.5 m over the year. The geological cross-section in Figure **2**A shows the non-saturated zone above the water table, which is composed of paleochannels of gravels and sands. This figure also shows the three hydrostratigraphic units defined at this site: (1) the upper part of the aquifer (UPA), which is also dominated by paleochannels of sands and gravels with interbedded layers of sands with fine matrix, although from the geological and textural point of view, this unit is homogeneous as a whole); (2) the lowermost part of the aquifer, which corresponds to the transition zone down to the bottom aquitard (TZBA, 2.30 m thickness), constitutes the sheet floods of the alluvial fans, and is a unit that geologically and texturally is highly heterogeneous, and is composed of numerous interstratified layers of millimeter and centimeter scale, formed by silty-clays between fine to coarse sands and gravels with variable fine matrix content; and (3) the bottom aquitard (BA), which is composed of red clays, at a depth of 14 m.

Figure **2**B displays the lithological, textural, and hydraulic conductivity differences between the UPA and TZBA (the weighted average hydraulic conductivities at B-S1UB were 160 and 1 m/d, respectively; and at B-S2UB, 230 and 4 m/d, respectively). Furthermore, large differences in transmissivity occur between the UPA and the TZBA (5.25 and 590 m^2/d, respectively). These differences in hydraulic conductivity and transmissivity derive from the different degree of geological and textural homogeneity-heterogeneity between both hydrostratigraphic units.The UPA and TZBA maintain their homogenous and heterogeneous character, respectively, throughout the monitored zone, as evidenced by the detailed analysis of stratigraphic logs of boreholes in the monitoring network (Figure **2**B). More information on the geological and hydrogeological framework is provided in the SD.

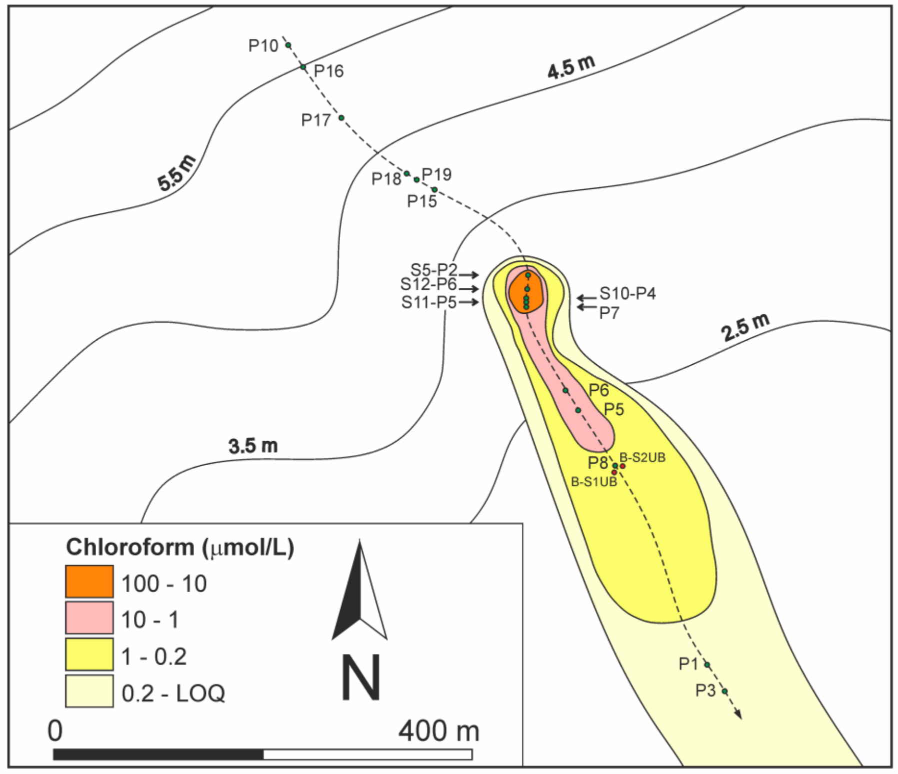

Figure 1. Water table map (in m above mean sea level) and contaminant CF plume. LOQ: limit of quantification. Dashed line: centerline of the source-plume (with the projection of piezometers that follow this line). B-S1UB and B-S2UB are the boreholes drilled to construct multilevel wells S1UB and S2UB, respectively.

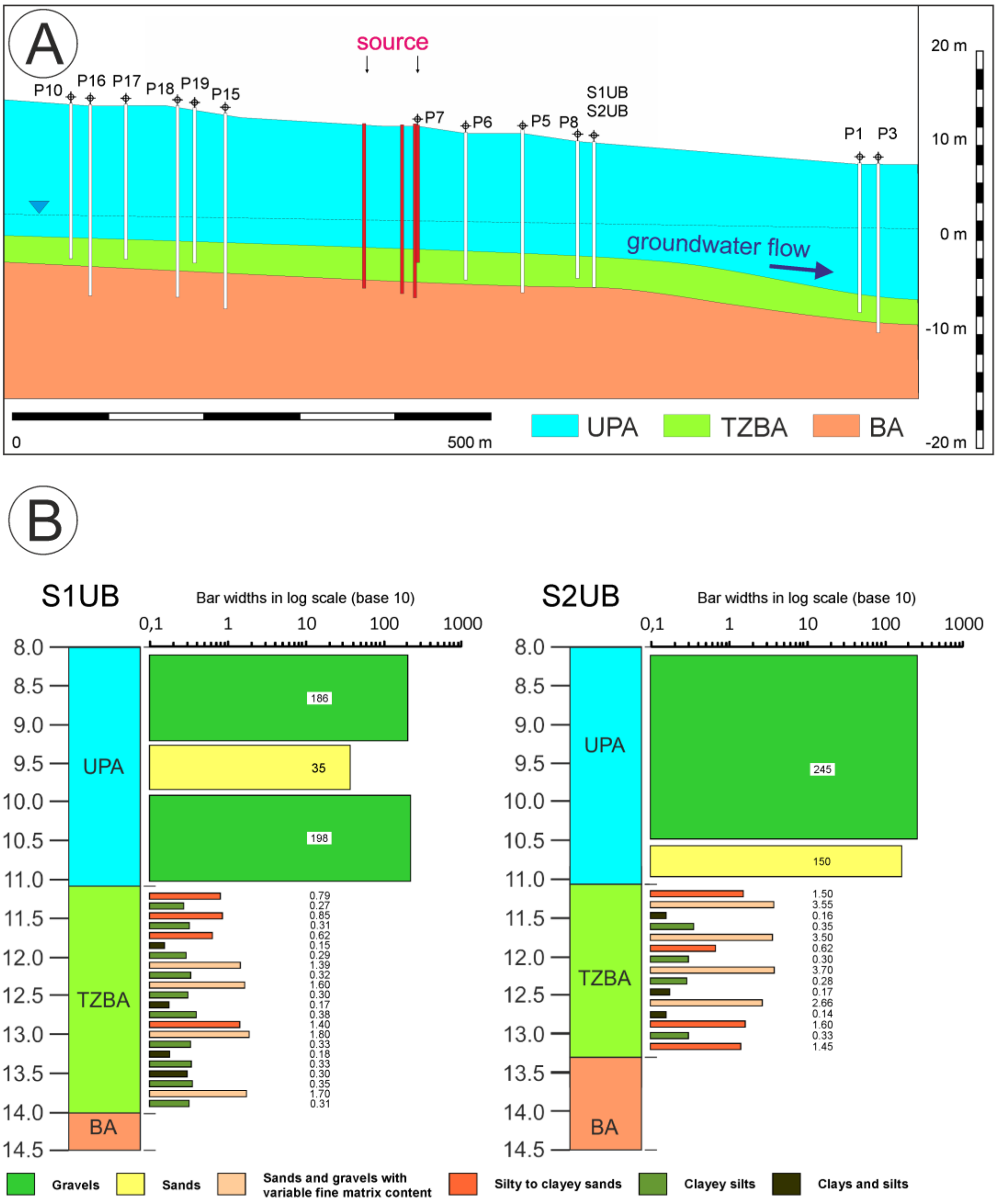

Figure 2. (A) Geological cross-section along the centerline of the plume showing the hydrostratigraphic units defined and piezometers and wells of monitoring network. (B) Variation with depth (m below ground) of the lithological and textural characteristics, and hydraulic conductivity (m/day) of the two studied hydrostratigraphic units (UPA and TZBA). Thickness of bars are the hydraulic conductivity (in a decimal log scale). BA (Bottom Aquitard).

4.2 Degradation processes and dominant redox conditions in the TZBA along the flow path

4.2.1 Eh values and redox-sensitive parameters and chloromethanes

A summary of the Eh values and concentrations of redox–sensitive parameters (DO, TOC, nitrate, nitrite, Mn^{2+}, Fe^{2+}, and sulfate) in the TZBA along the flow path, from upgradient of the main source to the front of the plume (Figure 1), is presented in Figure 3. This figure shows that the most highly reducing conditions occurred in the area of the main DNAPL source (Eh ranged between -63 and -134 mV, Figure 3A). Various elements converge in the main source area that make redox conditions highly anoxic in this area at the TZBA: i) the intrinsically high geological and textural heterogeneity in the TZBA, which implies a low hydraulic conductivity (see Section 4.1 and Figure **2**B) and little DO supply with groundwater flow; ii) the fact that a large portion of pores in the UPA and TZBA are occupied by DNAPL at different saturations (ITRC, 2015), leading to a greater decrease in hydraulic conductivity (Fetter, et al., 2017) and contributing even more to a decline in the supply of DO; and iii) the consumption of what little DO remains to oxidize the high TOC contents in groundwater (which ranged between 124.9 and 25.2 mg/L, Figure 3H) and particulate organic matter in subsurface sediments. The TOC values are consistent with the high organic carbon background associated with the petrochemical activities at the site reported by Puigserver et al. (2013). A non-negligible part of this background is formed by natural dissolved and particulate organic matter, as evidenced by groundwater and fine sediments sampled at the depth of the TZBA upgradient of the petrochemical complex).

Although nitrate and sulfate are two co-contaminants that cause diffuse contamination of groundwater across the whole region, their concentrations tended to decrease in the TZBA along the flow path upgradient of the source, with low λ and ε values of 0.00048 and 0.00032 m^{-1}, and -1.45 and -0.89‰ respectively for nitrate and sulfate. These λ values were lower than those along the flow path in the DNAPL source area (0.0039 and 0.0075 m^{-1}, and -8.66 and -7.88‰ respectively for nitrate and sulfate), where nitrite, Mn^{2+}, and Fe^{2+} tended to increase. All these elements agree with the mentioned redox conditions in the source area.

Low Eh and DO values were observed along the centerline of the plume in the TZBA (Figure 3A,B). This agrees with the high geological and textural heterogeneity of the TZBA throughout the site (Section 4.1), which leads to: i) low hydraulic conductivity and flow velocity, ii) little DO supply by groundwater, and iii) the consumption of this DO to oxidize the dissolved TOC and natural organic matter in the TZBA, giving rise to high anoxic conditions here and in the central part of the plume. This shows that geological and textural heterogeneity is the key control that accounts for the high anoxic conditions in the environment.

In contrast, Eh and DO values increased towards the periphery and frontal part of the plume, showing the input of DO by hydrodynamic dispersion, which agrees with the higher values of nitrate, sulfate, and TOC, and with the lower values of nitrite, Mn^{2+}, and Fe^{2+} in these parts.

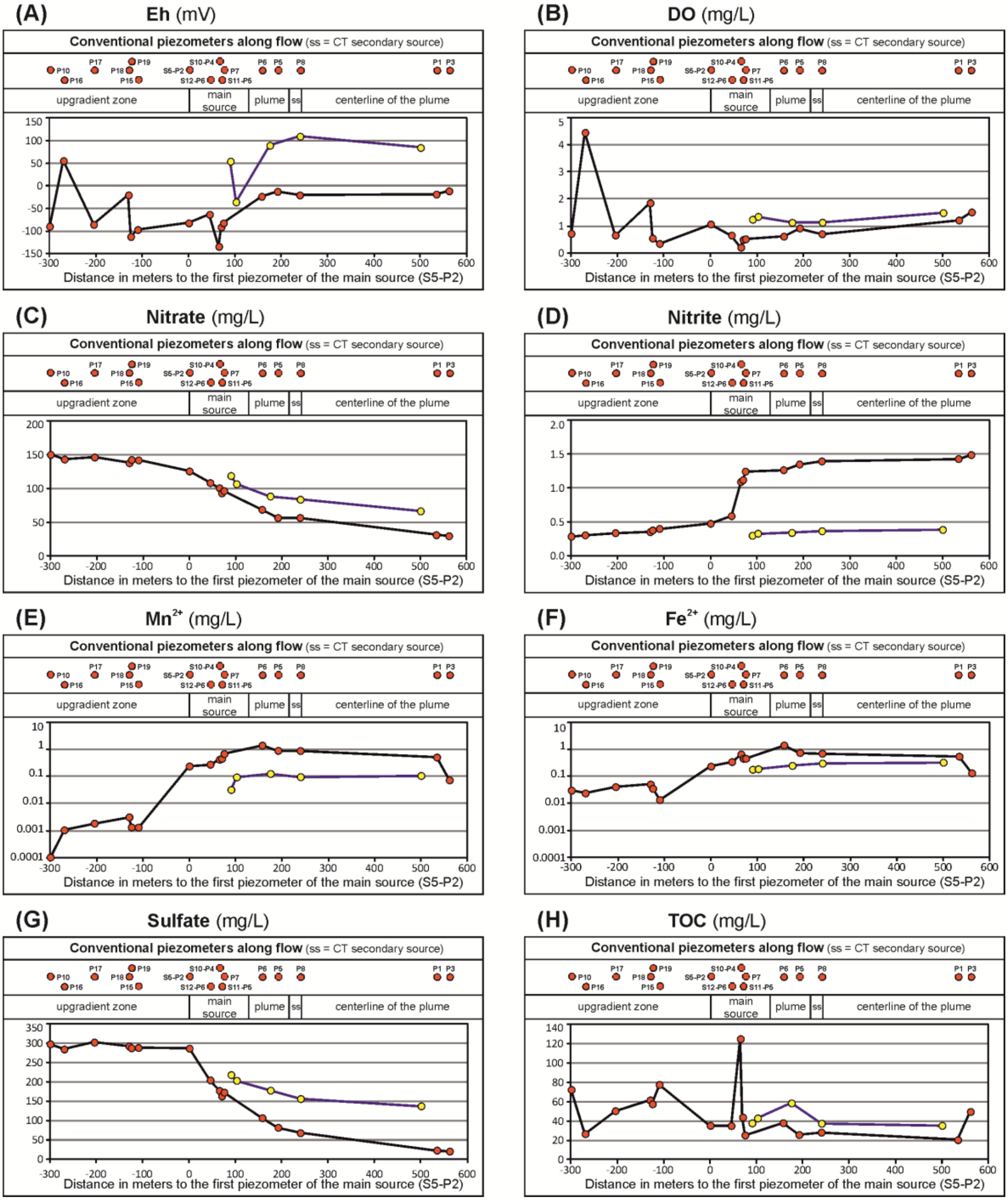

Figure 3. Summary of Eh values and concentrations of redox–sensitive parameters (DO, TOC, nitrate, nitrite, Mn^{2+}, Fe^{2+}, and sulfate) in the TZBA along the flow path (ss = CT secondary pool of DNAPL-source). Red line represents the centerline. Blue line is the average of peripheral zones.

Figure 4**¡Error! No se encuentra el origen de la referencia.** displays a summary of the concentrations of chloromethanes and isotopic compositions of CT and CF in the TZBA along the flow path. The highest concentration values of CT, CF, DCM, and CM were recorded principally at the main source. An increase in the concentrations of CT and CF occurred downgradient of the main source at piezometer P8 (Figure 4A,C). This finding reveals the existence of a small DNAPL pool, which is the secondary source mentioned in Section 2. This source is isolated from the area of the main DNAPL source and is located between piezometers P5 and P8.

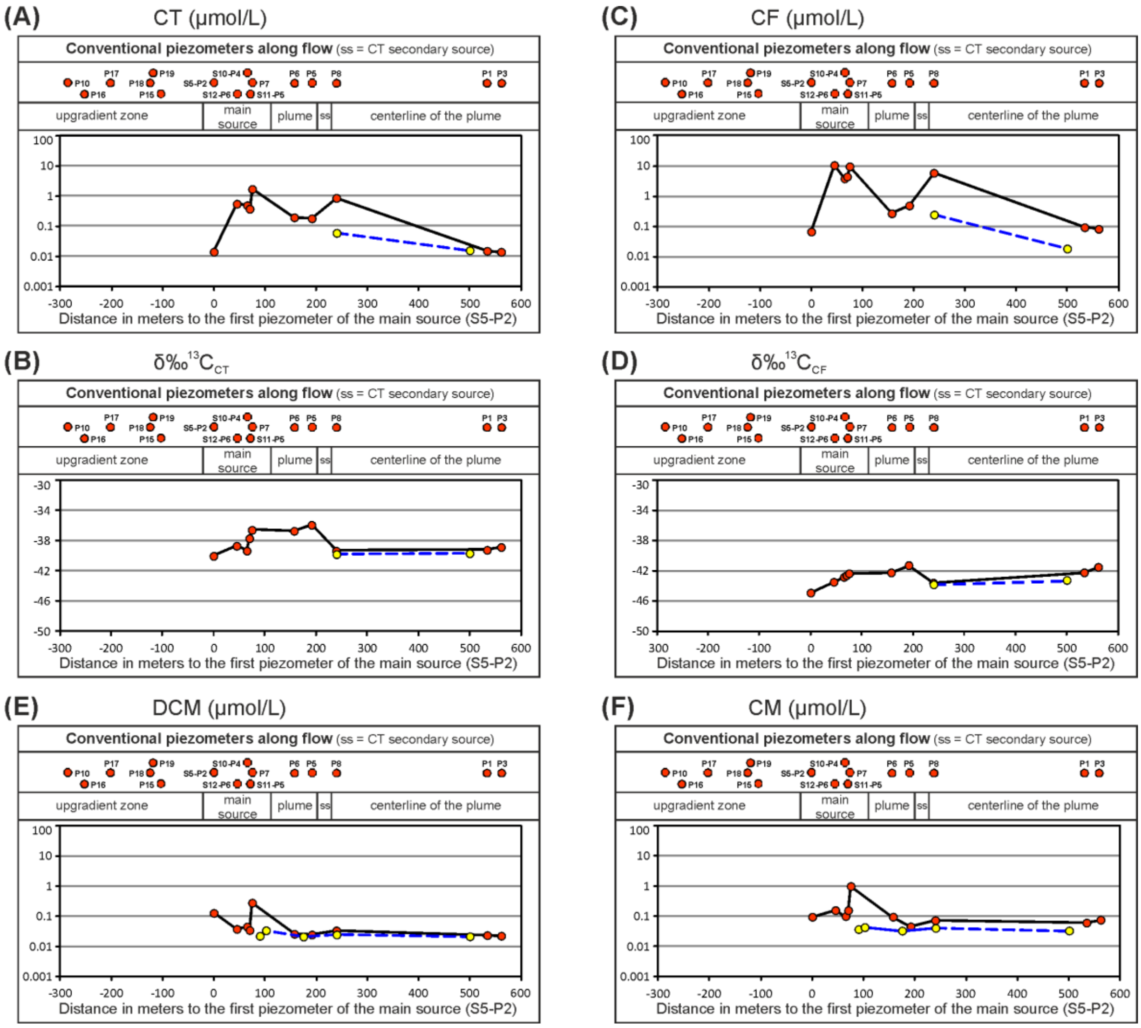

Figure 4. Summary of concentrations of chloromethanes and isotopic composition of CT and CF in the TZBA along the flow path (ss = CT secondary pool of DNAPL-source). Red line represents the centerline. Blue line is the average of peripheral zones.

4.2.2 Evidence of major degradation processes and dominant redox conditions

In this section, the major redox-dependent transformation processes occurring in the TZBA along the flow path are analyzed. The integration of these results allows determination of the dominant redox conditions.

Figure 5A shows that values of isotopic composition of nitrate fit to a denitrification line originated in the field of the use of manure as fertilizer. The dominant redox conditions in the zone upgradient of the source at the depth of the TZBA were denitrifying (Figure 6B), as denitrification was the only redox dependent process identified in this area. Nitrate and nitrite largely decreased and increased, respectively, in the TZBA along the flow path between the main and secondary source (Figure 3C,D). In addition, the heaviest $\delta^{15}N_{nitrate}$ and $\delta^{18}O_{nitrate}$ values in the conventional piezometers (27.14 and 21.82 ‰, respectively) were observed at the front of the plume. However, the highest attenuation rate of nitrate and isotope enrichment factor for ^{15}N along the flow path, occurred in the main DNAPL source area (with λ and ε values of 0.0039 m^{-1} and -8.66‰, respectively). All these results, as well as the increase in $Mn^{2+}$and Fe^{2+} (Figure 3E,F), the decrease in sulfate (Figure 3G), and the low Eh and DO values (Figure 3A,B), are evidence that reduction processes of nitrate occurred in the TZBAalong the flow path, especially along the main source area. The lower rate of attenuation and isotope enrichment factor observed for nitrate downgradient of the source along the centerline of the plume (λ and ε values of 0.0020 m^{-1} and -4.27‰) denoted that denitrification still occurred (Figure 6A).

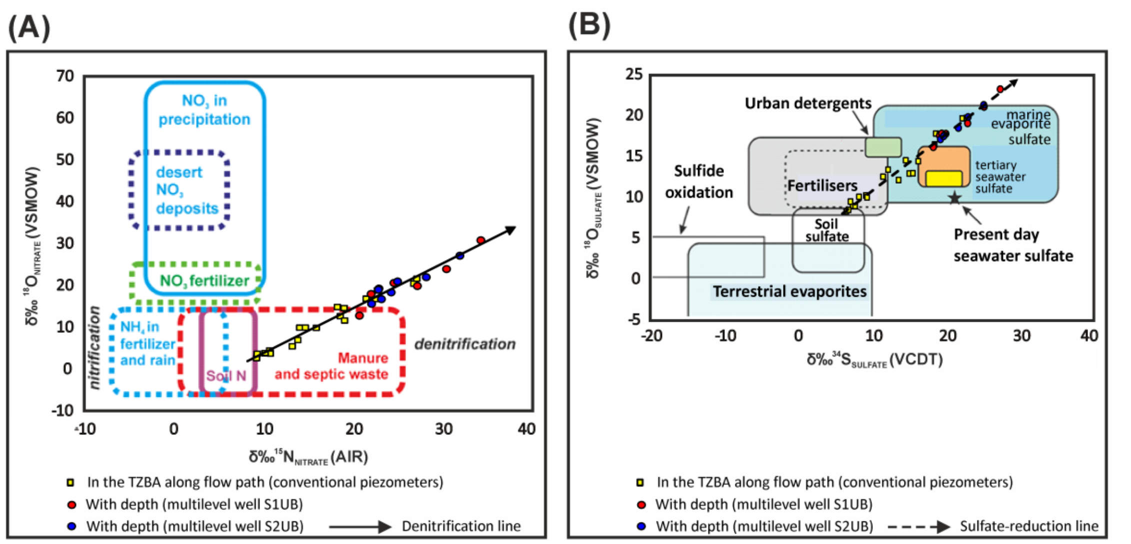

Figure 5. (A) Denitrification line in the TZBA along the flow path and with depth. (B) Sulfate-reduction line in the TZBA along flow path and with depth.

While Mn^{2+} and Fe^{2+} were low upgradient of the DNAPL source area (Figure 3E,F), with values that corresponded to background values, they increased in the source and immediately downgradient of this area. These observations, the low Eh and DO values (Figure 3B), and the reductive dechlorination and sulfate-reduction processes (see below) provide evidence that reduction occurred for the oxidized minerals of manganese and iron along the flow path in sediments of the TZBA (Figure 6A).

While CT and CF, and the other chloromethanes concentrations were below the LOQ in the TZBA along the flow path upgradient of the main source, a large increase was progressively recorded in the source area, where the highest values of CT and CF were recorded (Figure 4A,C). This increase was accompanied by the isotopic fractionation of these compounds (Figure 4B,D) as well as the formation of DCM and CM (Figure 4E,F), demonstrating that degradation of CT and CF occurred. A similar pattern of isotopic fractionation was observed downgradient of the main source, although the highest attenuation rates and isotope ε values of CT and CF in the TZBA along the flow path also occurred at the source, with λ values of 0.0684 and 0.0671 m^{-1}, respectively; and ε values of -3.58 and -2.67‰, respectively. Although δ^{13}C$_{CT}$ and

$\delta^{13}C_{CF}$ increased in the source area (Figure 4B,D), the aforementioned ε values, are underestimated since light CT is continuously dissolved from the CT contained in the DNAPL source and incorporated into the groundwater flow. As regards CF, the increase in fractionation of this compound, caused by its transformation into DCM, must be added to similar effects as those described for CT (i.e., light CF incorporating into groundwater from the CF contained in the DNAPL source) and by the CF proceeding from CT transformation. Given that the described degradation process of CT and CF occurred in parallel with the reduction of nitrate, natural oxidized manganese and iron minerals, and sulfate (see below), and consequently under highly anoxic redox conditions (see Section 4.2.1), it is plausible to affirm that it corresponds to reductive dechlorination of chloromethanes (Figure 6A). This process overlapped with the aforementioned biogeochemical process of denitrification, and despite the fact that the reduction potential of nitrate is greater than that of CT and CF, degradation of these compounds was not inhibited because of the highly anoxic conditions. The increase in CT that was observed between piezometers P5 and P8 (Figure 4**¡Error! No se encuentra el origen de la referencia.**A, i.e., in the secondary source, see Section 4.2.1) corresponded to an isotopic composition of this compound with a $\delta^{13}C_{CT}$ value of -39.30‰ in P8 (Figure 4**¡Error! No se encuentra el origen de la referencia.**B), which was similar to that of the main source in S5-P2 (-39.98‰). By contrast, the isotopic composition of CF in P8 ($\delta^{13}C_{CF}$ of -43.60‰, **¡Error! No se encuentra el origen de la referencia.**D) was heavier than that of the main source in S5-P2 ($\delta^{13}C_{CF}$ of -44.92‰). This finding suggests that the secondary pool is composed only of CT-DNAPL and that the increase in CF is caused by the degradation of CT. This pattern supports the fact that the DNAPL leaks originated from two different tanks, one for CT and the other for CF (see Section 2).

In the main DNAPL source, the ratio of the average molar concentration of CT to that of CF was 1 mole of CT per 9.25 moles of CF. By contrast, in the TZBA along the axial zone of the plume (and in its peripheral area, where conditions were not as reducing), the ratio was 1 mole of CT per 2.32 moles of CF. In addition, isotopic fractionation of CT was not recorded (Figure 4**¡Error! No se encuentra el origen de la referencia.**B), and low concentrations of DCM and CM were measured in the plume (Figure 4**¡Error! No se encuentra el origen de la referencia.**E,F), thus indicating a larger transformation of CT to CF (and successively, DCM and CM) in the source than in the plume (Figure 6A). By contrast, a decrease in the CF concentration (Figure 4**¡Error! No se encuentra el origen de la referencia.**C) accompanied by the isotopic fractionation of this compound (Figure 4**¡Error! No se encuentra el origen de la referencia.**D) occurred along the centerline of the plume, which gave rise to an attenuation rate and an isotope enrichment factor between conventional piezometer P7 (at the main source) and P3 (at the front of the plume) with λ and ε values of 0.0098 m^{-1} and -0.89‰, respectively.

Figure 5B shows that the $\delta^{34}S_{sulfate}$ and $\delta^{18}O_{sulfate}$ values fit a sulfate-reduction line originating in the sulfate-based fertilizers field). Sulfate largely decreased in the TZBA along the flow path between the main and secondary sources (Figure 3G). Moreover, the heaviest $\delta^{34}S_{sulfate}$ and $\delta^{18}O_{sulfate}$ values (22.75 and 19.80‰, respectively) were observed at the front of the plume. Nevertheless, as in the case of nitrate, CT, and CF, the highest rate of attenuation and enrichment factor for sulfate in the DNAPL source area were the highest (with λ and ε values of 0.0075 m^{-1} and -7.88‰, respectively). All these observations and the low Eh and DO values (Figure 3A,B) demonstrate that sulfate-reduction occurs along the flow path in the main source (Figure 6A) and downgradient in the plume, where the environment was highly anoxic (Figure 6B). This indicates that dominant redox conditions are sulfate-reducing in the source and the plume at the depth of the TZBA (Figure 6B), according to the thermodynamic model described by Christensen et al. (2000)(see Section 3.1).

The sulfate-reduction process requires more extreme reducing conditions than do the rest of the other processes occurring in the main source and the plume (Figure 6A). This accounts for the smaller concentrations of Fe^{2+} and Mn^{2+} and their smaller increase than those observed downgradient of the source (Figure 3E,F) since the precipitation of these metals in a reduced state occurs under these reducing conditions as carbonates and sulfides (rhodochrosite $MnCO_3$ and siderite $FeCO_3$; manganous sulfide MnS, ferrous sulfide FeS and pyrite FeS_2). A core sampling survey carried out by Puigserver et al. (2013) in boreholes B-S1UB and B-S2UB registered high values of Mn and Fe in sediments of the TZBA at depths similar to those of the source of CT and CF, which could be evidence of precipitation of the Mn and Fe minerals.

At the depth of the TZBA, the rate of attenuation observed for sulfate downgradient of the source was lower than at the source (λ value of 0.0030 m^{-1}), demonstrating that the sulfate-reduction process still occurred in the plume (Figure 6A), and even in the peripheral zone (Figure 3G), regardless of the environment was less anoxic because Eh and DO progressively increased (Figure 3A,B).

In summary, the dominant sulfate-reducing redox conditions control the processes occurring along the flow path at the depth of the TZBA in the study site, including the reductive dechlorination of CT and CF (Figure 6B). This process takes place at a very high rate in the main DNAPL source in a highly anoxic environment (Figure 6B, with DO ranging between 0.20 and 0.65 mg/L). The high geological and textural heterogeneity in the TZBA (see Section 4.1) that led to low DO supply and its subsequent consumption in the oxidization of the dissolved TOC and natural organic matter in fine sediments, gave rise to the anoxic conditions (see Section 4.2.1) that favored the reductive dechlorination of chloromethanes.

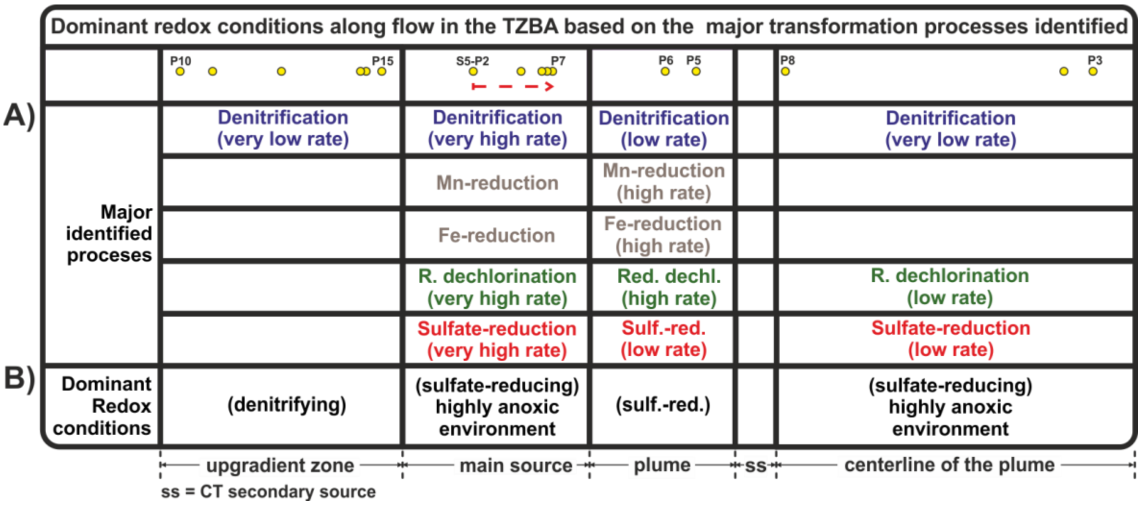

Figure 6. Major identified processes and dominant redox conditions in the TZBA along the flow path. Analyses based on results shown in Figure 3, Figure 4 and Figure 5. Possible precipitation of carbonate and sulfide minerals of Mn and Fe could occur in the main source.

4.3 Degradation processes and dominant redox conditions with depth

The following is a detailed perspective of two biogeochemical profiles of groundwater depth in the UPA and TZBA, obtained in the two multilevel wells (S1UB and S2UB) located in the axis of the chloromethanes plume 220 m downgradient of the main DNAPL source (Figure 1).

4.3.1 Eh values and redox-sensitive parameters and chloromethanes

A summary of the variation of Eh values and concentrations of redox-sensitive parameters (DO, TOC, nitrate, nitrite, Mn^{2+}, Fe^{2+}, and sulfate) with depth is shown in Figure 7. Eh and DO decreased at the depths of the UPA (ports 1 to 4, Figure 7A,B), which is consistent with reducing conditions and with the fact that nitrate and sulfate concentrations decreased and nitrite, Mn^{2+}, and Fe^{2+} increased (Figure 7). However, the most highly anoxic conditions occurred at depths of the TZBA (ports 5 to 7), with an average Eh value of -24 mV, which coincided with a high average TOC value of 32.4 mg/L, whose oxidation favored DO consumption. This TOC content was close to that of the average values of conventional piezometers P5 and P8 at the depth of the TZBA (27.4 mg/L), which are nearby S1UB and S2UB. As in the source, TOC concentrations in the plume agree with the high organic carbon background at the site and with the abundant natural particulate and dissolved organic matter in the numerous interbedded layers of fine material of the TZBA, which again denotes that the great geological and textural heterogeneity of this hydrostratigraphic unit is the key control that gives rise to highly anoxic conditions (similar to those at the main source, see Section 4.2.1). Under these highly anoxic conditions, concentrations of nitrate and sulfate decreased from port 5 to 7 (Figure 7D,E; with average values of 28.8 mg/L and 38.3 mg/L, respectively), whereas nitrite, Mn^{2+} and Fe^{2+} tended to increase (Figure 7F,G,H; with average values of 1.9 mg/L, 1.3 mg/L, and 2.4 mg/L, respectively).

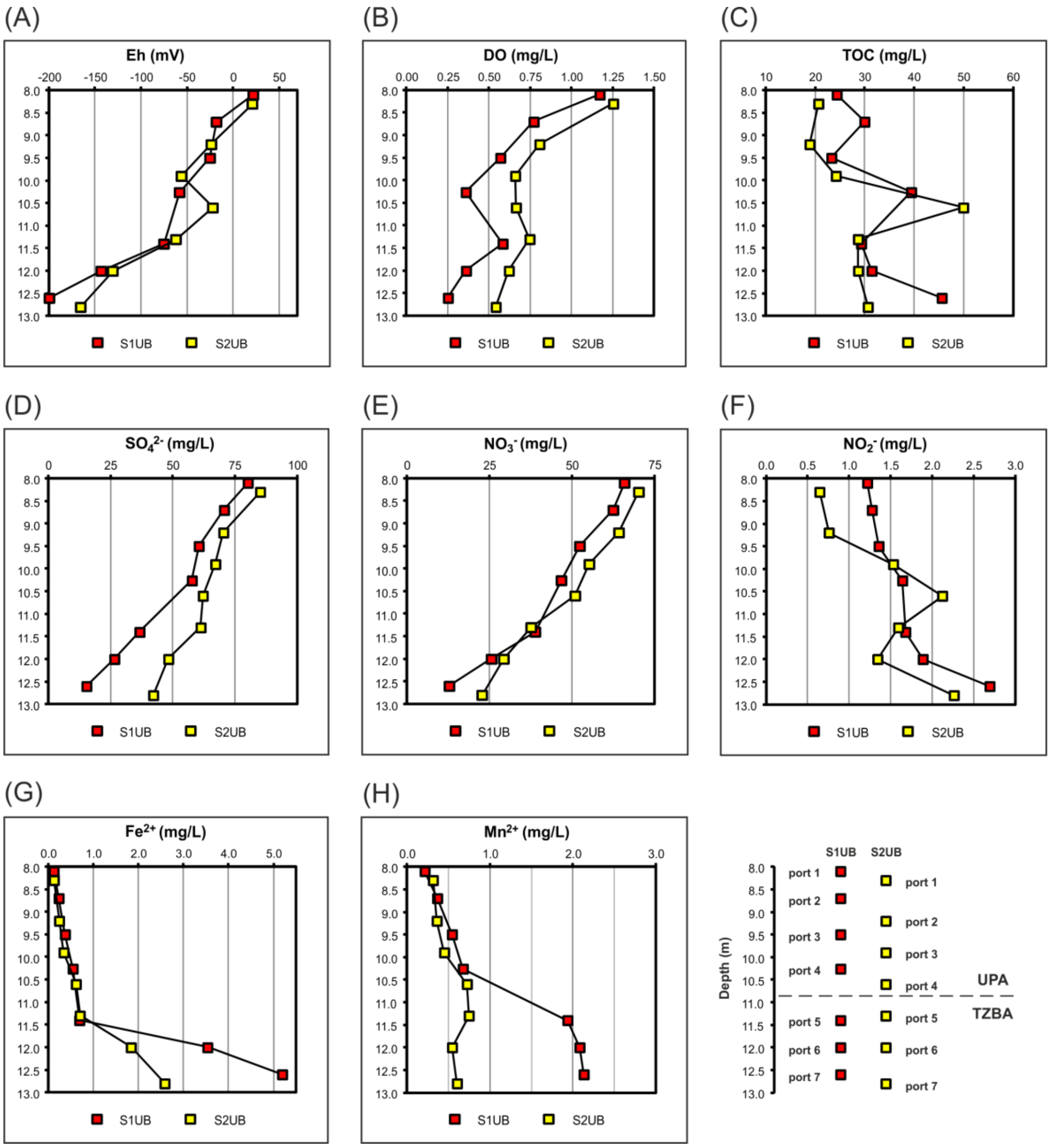

Figure 7. Variation of Eh values and concentrations of redox–sensitive parameters (DO, TOC, nitrate, nitrite, Mn^{2+}, Fe^{2+}**,** and sulfate) with depth. UPA (Upper Part of the Aquifer). TZBA (Transition Zone to the BottomAquitard).

As for chloromethanes, Figure 8 displays a summary of their concentrations and the isotopic composition of CT and CF with depth. The highest values of CT were found at the top of the TZBA (port 5), whereas the highest values of CF, DCM, and CM were recorded at the bottom of this unit (ports 6 and 7).

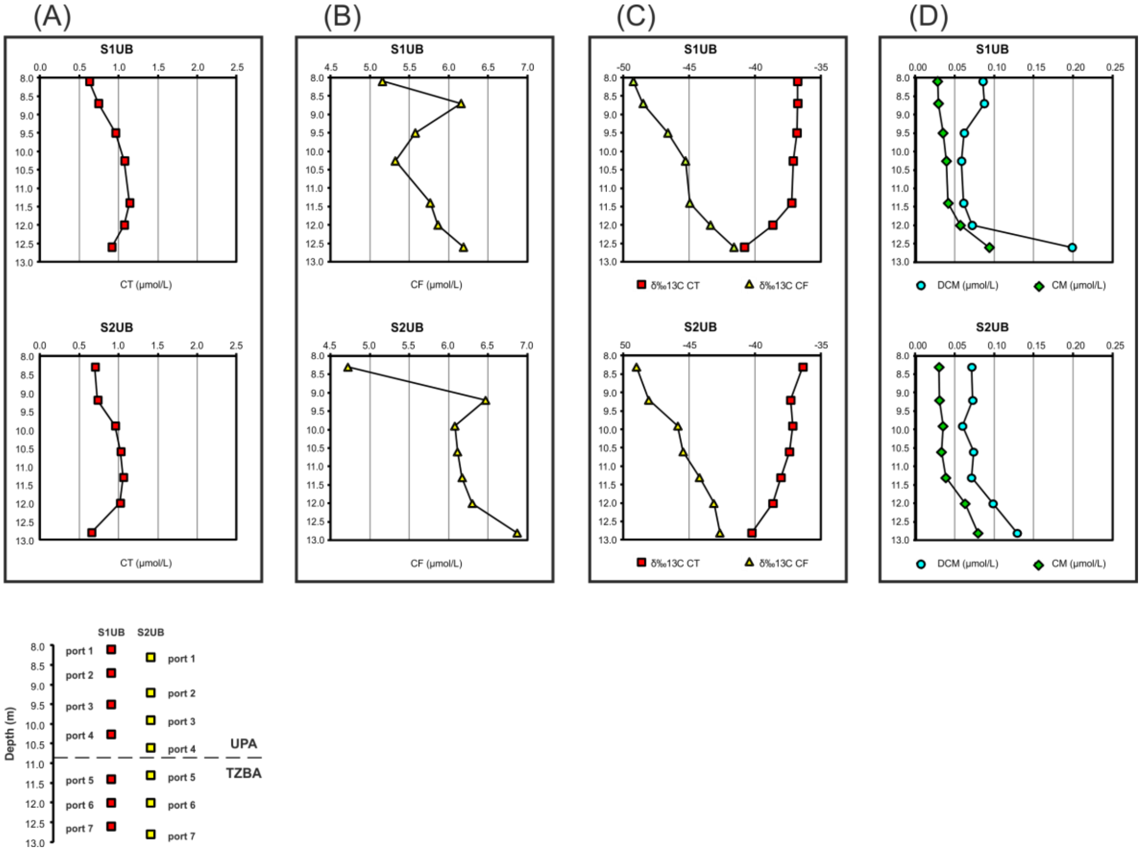

Figure 8. Variation of concentrations of chloromethanes and isotopic composition of CT and CF with depth. UPA (Upper Part of the Aquifer). TZBA (Transition Zone to the Bottom Aquitard).

4.3.2 Evidence of major degradation processes and dominant redox conditions

Figure 9A shows the major redox-dependent transformation processes that occurred and the redox conditions that were dominant with depth in the UPA and TZBA (Figure 9B).

As with along the flow path in the TZBA, denitrification of nitrate was recorded with depth (Figure 5A). The vertical concentration profiles of nitrate and nitrite (Figure 7E,F) showed a higher decrease of nitrate and an increase of nitrite in the TZBA (ports 5 to 7) compared to those in the UPA (ports 1 to 4), where denitrification from the zone upgradient of the DNAPL source to ports of multilevel wells in the plume occurred at a lower attenuation rate and isotope enrichment factor than in the TZBA (with λ of nitrate and ε for^{15}N values of 0.0037 and 0.0069 m^{-1}, and -13.38 and -19.91‰, respectively in the UPA and TZBA). All these results, in addition to the increase in Fe^{2+} (Figure 7G), the decrease in sulfate (Figure 7D), and the low Eh and DO values in the depth profile of the TZBA (Figure 7A,B), are evidence that, although denitrification, does occur in the UPA, this process is more relevant in the TZBA (Figure 9B).

The Fe^{2+} and Mn^{2+} concentrations varied little in the UPA, but increased in the TZBA, especially Fe^{2+}, indicating the occurrence of Fe-reduction processes (Figure 9A).

In multilevel wells S1UB and S2UB, gradual increases in CT from port 1 to 4 in the UPA and decreases from 5 to 7 in the TZBA (Figure 8A) were recorded. As reported by Puigserver et al. (2013) at this site, these maximums in groundwater coincided with two CT concentration peaks in the PWFS of boreholes B-S1UB and B-S2UB, which were caused by the secondary small DNAPL pool of CT (see Section 4.2.1). Although CT in groundwater decreased in the TZBA, $\delta^{13}C_{CT}$ values also decreased with depth (Figure 8C), demonstrating that the input of dissolved CT from the secondary pool (which is isotopically light) masks the isotopic fractionation of this compound in groundwater in ports 5 to 7 of the TZBA. The CF concentrations and $\delta^{13}C_{CF}$ values increased with depth in ports 1 to 4 of the UPA (Figure 8B,C). This isotopic fractionation of CF in the UPA was accompanied by a slight increase in the DCM concentration, along with the formation of CM (Figure 8D). As for the TZBA, an increase in CF, DCM, and CM was detected, along with isotopic fractionation of CF (Figure 8B,C,D). Furthermore, the variation of concentrations of chloromethanes in groundwater at the TZBA occurred in parallel to a similar variation of these compounds in PWFS (Puigserver et al., 2013), particularly in sediments found at the depth of port 7 of multilevel wells. All these elements and the increase with depth of CF, DCM, and CM in ports 5 to 7 of the TZBA, as well as the sulfate-reducing conditions prevailing in the TZBA along the flow path (see Section 4.2.2) and with depth (see below), are evidence that the reductive dechlorination of CT and CF (and of DCM) is a more substantial process in the TZBA than in the UPA, with higher attenuation rates and isotope ε values for CT and CF from the source zone to ports 5 to 7 of multilevel wells in the TZBA (λ and ε of 0.0044 m^{-1} and -3.42‰, respectively for CT, and of 0.0045 m^{-1} and -2.72‰, respectively for CF) than in the UPA in ports 1 to 4 (λ and ε of 0.0029 m^{-1} and -0.81‰, respectively for CT, and of 0.0006 m^{-1} and -1.15‰ for CF, respectively).

As along the flow path, sulfate evolution with depth showed that the sulfate-reduction process also occurred (Figure 5B). The sulfate variation from the zone upgradient of the DNAPL source to the plume at depths in the sampling ports in the multilevel wells, registered a greater decrease at ports 5 to 7 in the TZBA than at ports 1 to 4 in the UPA (Figure 7D). These differences correspond to different attenuation rates and enrichment factors between the two hydrostratigraphic units, with higher attenuation rate and isotope enrichment factor in the TZBA than in the UPA (λ of sulfate and ε for ^{34}S values of 0.0085 and of 0.0060 m^{-1}, and -17.10 and -12.63‰, respectively).

As in the main DNAPL source (see Section 4.2.2), groundwater of ports 5 to 7 in the TZBA showed dominant sulfate-reducing redox conditions in an environment that was more anoxic than in the UPA (Figure 9B). All these results, along with the increase in Fe^{2+} (Figure 7G), the decrease in sulfate, and the low Eh and DO values (Figure 7A,B), reveal that although sulfate-reduction also occurs in the UPA, this process is particularly noteworthy in the TZBA.

This highly anoxic environment in the TZBA explains the very low increases in Mn^{2+}concentrations in the TZBA compared to the UPA (Figure 7H), since manganese in a reduced state could precipitate as carbonate (rhodochrosite $MnCO_3$) and as manganous sulfide (MnS). Evidence of precipitation of Mn minerals could be the high aforementioned Mn values in sediments along the flow path at the depth of the TZBA (see Section 4.2.2).

In summary, depth profiles obtained with multilevel wells S1UB and S2UB in the TZBA confirm that reductive dechlorination of CT and CF is controlled by the dominant sulfate-reducing redox conditions (as was observed along the flow path in the zone of the plume close to conventional piezometer P8). Moreover, these profiles allow affirming that these redox conditions occur in a highly anoxic environment (Figure 9B), since DO contents from ports 5 to 7 (Figure 7B) varied between 0.25 and 0.75 mg/L. As is the case along the flow path, the great geological and textural heterogeneity in the TZBA is the key control that accounts for the very low DO content (see Section 4.2.1), and consequently, also for the sulfate-reducing conditions and the highly anoxic environment.

These conditions are close to those along the flow path in the main source area (Figure 6B). Accordingly, attenuation rates and isotope enrichment values of CT with depth in the TZBA (λ and ε calculated between the maximum concentration in the source (piezometer P7) and ports of multilevel wells in the TZBA, see Section 3.1) were close to those in the main source along the flow path (λ and ε with depth of 0.0044 m^{-1} and -3.42‰, respectively; and λ and ε in the main source of 0.0684 m^{-1} and -3.58‰, respectively, see Section 4.2.2). Similarly, for the case of CF, attenuation rates and isotope enrichment were close to those of the main source (λ and ε with depth of 0.0045 m^{-1} and -2.72‰, respectively; and λ and ε of 0.0671 m^{-1} and -2.67‰, respectively, see Section 4.2.2).

By contrast, attenuation rates (Figure 9A) and isotope enrichment values of CT and CF were higher in the TZBA than in the UPA. Thus, λ and ε values of 0.0044 m^{-1} and -3.42‰, respectively for CT; and 0.0045 m^{-1} and -2.72‰, respectively for CF were obtained in the TZBA; whereas, λ and ε values of 0.0029 m^{-1} and -0.81‰, respectively for CT; and 0.00406 m^{-1} and -1.15‰, respectively for CF were obtained in the UPA.

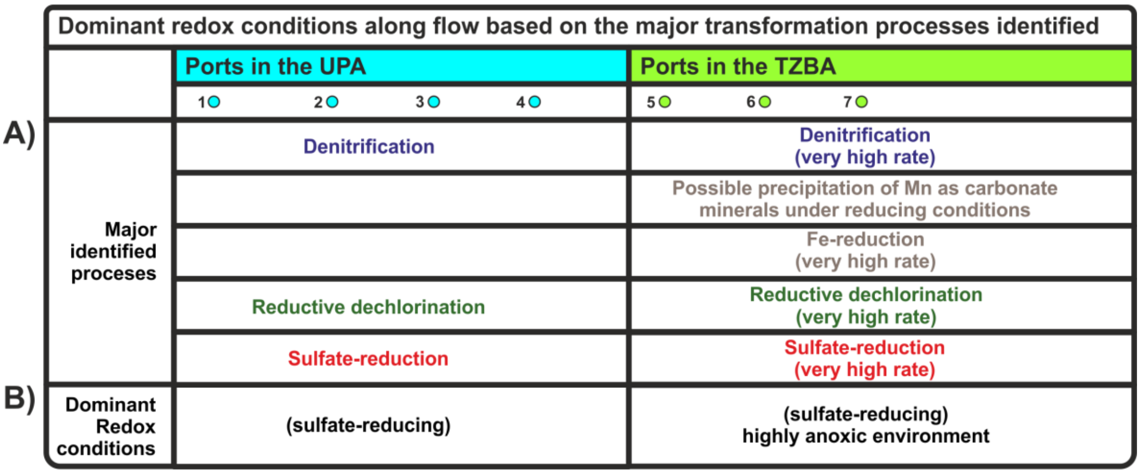

Dominant redox conditions along flow based on the major transformation processes identified

		Ports in the UPA	Ports in the TZBA
		1○ 2○ 3○ 4○	5○ 6○ 7○
A)	Major identified proceses	Denitrification	Denitrification (very high rate)
			Possible precipitation of Mn as carbonate minerals under reducing conditions
			Fe-reduction (very high rate)
		Reductive dechlorination	Reductive dechlorination (very high rate)
		Sulfate-reduction	Sulfate-reduction (very high rate)
B)	Dominant Redox conditions	(sulfate-reducing)	(sulfate-reducing) highly anoxic environment

Figure 9. Major identified processes and dominant redox conditions with depth. Analysis based on results shown in Figure 7and Figure 8. Possible precipitation of carbonate and sulfide minerals of Mn could occur in the TZBA.

4.4 Microbe diversity and abundance in groundwater and PWFS with depth

Analyses of the DGGE profiles of the set of samples of groundwater and PWFS uncovered a total of 29 bands (results on diversity and abundance in each DGGE profile are referred to this quantity, Table 1). Of these, the profiles of groundwater in the UPA showed in general greater average diversity and abundance (i.e., greater number of bands and greater brightness of bands, respectively of microbial communities in this hydrostratigraphic unit than in the TZBA, Table 1). This finding supports that the top of the UPA, which is found immediately below the water table oscillation zone, constitutes an ecotone in the subsurface (i.e., a natural zone where exchanges between two ecological systems of adjacent microbial communities occur), as demonstrated by Goldscheider et al. (2006) in unconfined aquifers. Furthermore, a large microbial diversity (value of 13), detected at port 3 of S1UB (central part of the UPA at 9.50 m deep), coincided with high microbial diversity (value of 6) in the PWFS sampled at a similar depth in borehole B-S1UB (sample M1 at 9.61 m depth), where a geological contact between coarse and fine materials occurred.

In the TZBA, the contact surfaces between the different texture materials also constitute ecotones (as described by Goldscheider et al., 2006). However, as mentioned above, a decrease in the average diversity and abundance was observed with depth in groundwater compared to what was observed in the UPA (Table 1). This decrease was more drastic in the TZBA of S1UB than in S2UB, which is consistent with the lower grain size in S1UB (and accounts for its lower hydraulic conductivity, see Section 4.1 and Figure 2B), as reported by Puigserver et al. (2013) for this site. The high amount of fine sediments and the variable matrix content of coarser sediments in the TZBA (see Section 4.1) makes it convenient to compare the grain size and average diameter of pore throats with the size of microorganism cells in the subsoil. Thus, the classical sedimentological literature provides grain sizes smaller than 2 µm for clays, and sizes ranging from 2 to 50 µm for silts. Moreover, Shuangfang et al. (2018), in a study on pore throat diameters in fine sediments, reported diameter values ranging from 0.09 to 0.86 µm for clayey and silty sediments, which are coherent with grain sizes of fine sediments. The maximum of this range of pore throat diameters, rounded to 0.9 µm, could be considered as the pore throat threshold that inhibits the migration of bacteria through groundwater. The results recorded by different authors for the size of most subsoil cell bacteria range between 0.2 and 5 µm (Alexander, 1978; Amodu, Ojumu and Ntwampel, 2013; Portillo et al., 2013; Joergensen and Wichern, 2018). The pore throat threshold diameter of 0.9 µm is greater than the value of 0.2 µm, corresponding to the size of the smallest cells. This is why a considerable portion of microorganisms (those greater than 0.9 µm) are physically unable to penetrate into the fine sediments and into the fine matrix of coarse sediments and in the TZBA, which accounts for the decline in diversity and abundance observed in multilevel wells in this unit (Table 1).

This is an important outcome for any contamination scenario in the subsoil, because biostimulation or bioaugmentation actions cannot be conducted if a significant part of the microorganisms living in the aquifer cannot penetrate the fine sediments of the transition zone (or the fine sediments at other depths in the aquifer). The relevance of this lies in the need to verify whether the microorganisms proposed to biostimulate, or those that are intended to be introduced in bioaugmentation actions, can migrate through the finest subsoil materials before implementing such remediation strategies.

In the case of the site studied, Figure 10A,B,C,D shows that the two microorganisms involved in the degradation of CT and CF (see Section 4.5) are small enough to flow with groundwater and, in the case of *A. suillum*, to penetrate into the PWFS in the TZBA (Figure 10C).

In summary, from the point of view of the structure of microbial communities, the geological and textural heterogeneity is one of the elements that determine the diversity and abundance of microorganisms in the subsurface. In addition, these heterogeneities, especially textural heterogeneity, are factors that condition the penetration of dechlorinating microorganisms into fine and less-conductive materials of the TZBA, where they are responsible for the natural attenuation of CT and CF (see Section 4.5.2), which penetrated via molecular diffusion into the less fine and less-conductive materials.

			Diversity (average values)		**Abundance** (average values)
			A	**B**	**C**
		Hydrostratigraphic unit	**Number of bands in profiles**	**Percentage values (%)**	**Brightness intensity of bands in profiles (on a 0-100 scale)**
Multilevel wells (GW)	**S1UB**	**UPA**	7.5	25.86	42.78
		TZBA	3.7	12.64	34.99
	S2UB	**UPA**	5.3	18.10	43.08
		TZBA	5.0	17.24	36.73
Boreholes (PWFS)	**B-S1UB**	**UPA**	3.5	12.05	46.60
		TZBA	5.0	17.24	40.60
	B-S2UB	**UPA**	2.8	9.66	40.87
		TZBA	2.0	6.90	34.82

Table 1. Average values of diversity and abundance of microbial communities in the two studied hydrostratigraphic units. Values obtained from analysis of DGGE profiles of groundwater samples in multilevel wells S1UB and S2UB and PWFS in boreholes of these multilevel wells.

4.5 Microorganisms involved in the degradation of CT and CF

4.5.1 Identification of OTU 6 and OTU 15 in the upper part of the aquifer

The combination of DGGE results with those of the clone library analysis (see Section 3.2 and the SD) allowed identification of the band corresponding to *A. suillum* (OTU 6) in the groundwater of all S1UB ports in the UPA (ports 1 to 4, Figure 10A). This indicates that *A. suillum* is a planktonic microorganism transported into the groundwater flow (like many bacteria in the subsurface ecosystem, Herrmann et al., 2019) that probably comes from areas located upgradient of the DNAPL source, even from beyond the petrochemical complex. By contrast, this band was only present in ports 2 and 4 in S2UB, although their abundance was similar in the two multilevel wells (Figure 10A). OTU 6 was not identified in the DGGE profiles of PWFS in B-S1UB and B-S2UB (in that case, in the fine matrix of interbedded sands collected at the UPA, Figure 10C). The cause of this absence is the small portion of fine matrix in these sands, which prevents the accumulation of this microorganism inside the matrix (see below Section 4.5.2).

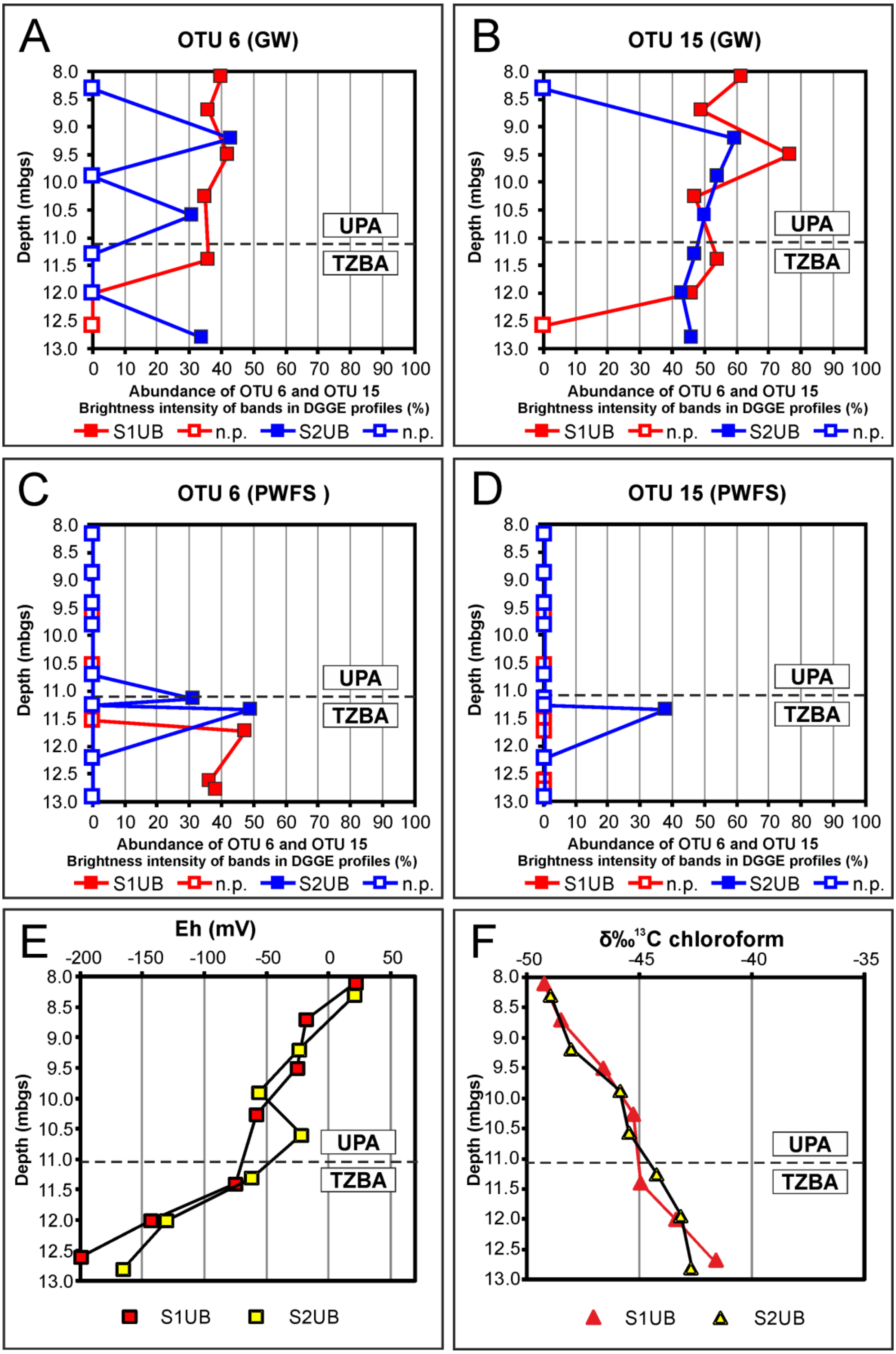

Figure 10. Abundance of OTU 6 (*A. suillum*) and OTU 15 (Clostridiales bacterium). (A) and (B), in groundwater samples in multilevel wells. (C) and (D) in porewater of fine sediment samples. “np” = not presence of the microorganism. (E) and (F) Variation of Eh and isotopic composition of CF, respectively.

The presence of OTU 6 in the groundwater of UPA (Figure 10A) coincided with the following: (1) an increase of CT with depth (Figure 8A) due to the dissolution of the secondary source of CT (see Section 4.2.2) and a decrease of the $\delta^{13}C_{CT}$ value (Figure 8C) due to the input of unfractionated CT from the secondary source; and (2) the denitrification and sulfate-reduction processes with depth (Figure 6A; see Section 4.3.2). The presence of OTU 6 and the occurrence of denitrification agree with Achenbach et al. (2001), who reported that *A. suillum* uses nitrate as an electron acceptor.

As for the bacterium of the order Clostridiales (OTU 15) in the UPA, this microorganism was present in all ports of S1UB in this hydrostratigraphic unit (ports 1 to 4) and in almost all of S2UB (Figure 10B); hence, it is also a planktonic microorganism. Moreover, OTU 15 presented greater abundance in the two multilevel wells than did OTU 6 (Figure 10B). The presence of OTU 15 in the groundwater of this unit coincided with: (1) an increase in the $\delta^{13}C_{CF}$ value (Figure 10F) and the presence of DCM (Figure 8D), which are elements supporting the reductive dechlorination of CF in the UPA; and (2) the aforementioned denitrification process with depth (Figure 9A) under sulfate-reducing dominant redox conditions (Figure 9B) with Eh values progressively more negative (Figure 10E). These findings agree with those of Grostern et al. (2010), Chan et al. (2012), and Justicia-Leon et al. (2014), who reported that the Clostridiales order of bacteria includes the genus *Dehalobacter*, which gives rise to reductive dechlorination of CF (and isotopic fractionation of this compound) to form DCM. Furthermore, Justicia-Leon et al. (2014) demonstrated that the biodegradation of CF to DCM occurs under anoxic conditions, including those of denitrification. Similar to the case of OTU 6, OTU 15 was not identified in the sediment samples collected in the UPA in B-S1UB and B-S2UB. Furthermore, it was only present in one sample in the TZBA (Figure 10D), which indicates that, unlike *A. suillum*, the ability to penetrate the fine materials of the Clostridiales microorganism was hindered, probably because of a .cell size larger than the pore throat threshold diameter value of 0.9 μm (see Section 4.4).

4.5.2 Role of OTU 6 and OTU 15 in degrading CT and CF in the transition zone

The band corresponding to *A. suillum* (OTU 6) was only identified in port 5 of S1UB and port 7 of S2UB in the groundwater at the TZBA (Figure 10A), which again shows that *A. suillum* is a planktonic microorganism (see Section 4.5.1). In contrast, this band was identified at several depths in the DGGE profiles of PWFS in this unit (Figure 10C) and with a greater abundance than that in groundwater ports 5 of S1UB and 7 of S2UB (Figure 10A), which is evidence that the cell size of *A. suillum* is small enough to penetrate into the finest sediments (see Section 4.4**¡Error! No se encuentra el origen de la referencia.**), where it accumulates and remains attached to the surface of mineral grains. This microorganism is an anaerobic, nitrate-dependent bacterium that rapidly uses the Fe(II) content of natural sediments as an electron donor under anoxic conditions and nitrate as the electron acceptor (Achenbach et al., 2001) to produce mixed-valence Fe(II)-Fe(III) byproduct precipitates, which are unstable iron minerals that correspond to green rusts (Chaudhuri et al., 2001; Lack et al., 2002; Weber et al., 2006; Nam et al.; 2016). Studies by different authors have confirmed the abiotic reductive dechlorination process of CT in the presence of green rusts (Liang and Butler, 2010; Yin et al., 2017), which are common natural electron donors in aquifers (Matocha, Dhakal and Pyzola, 2012) capable of degrading CT to CF, DCM, CM, and CH_4 (O'Loughlin, Kemner and Burris, 2003). Although the occurrence of green rusts was not determined in the present study, the following indirect indications that suggest their occurrence and role as natural reducing agents of CT to form CF were confirmed in the TZBA: (1) *A. suillum* was present, especially in the PWFS of the TZBA (with an abundance greater than that in the UPA, Figure 10C); (2) the very high denitrification rate and enrichment factor (λ and ε values of 0.0069 m^{-1} and -19.91‰, respectively) and the Fe-reduction of iron oxidized minerals, which delivers Fe^{2+} to the environment (Figure 7G); (3) the decrease of CT in groundwater (Figure 8**¡Error! No se encuentra el origen de la referencia.**A, from ports 5 to 7) and in the fine sediments (data shown in Puigserver et al., 2013); (4) the high values in the attenuation rate and enrichment factor of CT in the TZBA (λ and ε of 0.0044 m^{-1} and -3.42‰, respectively), which contrast with those of CT in the UPA (0.0029 m^{-1} and -0.81‰); (5) the increase of CF in groundwater in ports of the two multilevel wells at the TZBA (Figure 8**¡Error! No se encuentra el origen de la referencia.**B) and in fine sediments at a similar depth to that of ports 6 and 7 of this unit (Puigserver et al., 2013); (6) the high rate of sulfate-reduction and enrichment factor (λ and ε of 0.0085m^{-1} and -17.10‰, respectively); and (7) the dominant sulfate-reducing redox conditions (Figure 9B) and highly anoxic environment at the TZBA (Figure 10E) as a consequence of the intrinsically high geological and textural heterogeneity in this hydrostratigraphic unit (see Section 4.3.1).

All these indications are consistent with the precipitation of green rusts that are biogenically formed by *A. suillum*, and the subsequent abiotic reductive dechlorination of CT by the green rust. Thus, the reductive dechlorination of CT observed in the TZBA would correspond to an abiotic process that was biogenically mediated by *A. suillum*.

With respect to the bacterium of the order Clostridiales in the TZBA, it is reasonable to refer again to the genus *Dehalobacter* mentioned in Section 4.5.1. In this section, the authors reported that *Dehalobacter* is a genus of the order Clostridiales capable of giving rise to reductive dechlorination of CF, accompanied by isotopic fractionation, to form DCM. This finding agrees with the laboratory-scale observations of Puigserver et al. (2016c) and with the field-scale observations of the present study, in which a bacterium of the order Clostridiales was involved in the biotic reductive dechlorination of CF to form DCM and CM (Figure 8D).**¡Error! No se encuentra el origen de la referencia.**

4.6 Key control of heterogeneity in the TZBA on the NA of CT and CF

A sequence of successively dependent factors representing the conceptual model of the fate of CT and CF in the TZBA (Figure 11) reveals that the high geological and textural heterogeneity in the TZBA compared to the homogeneity in the UPA is the most important key control exerted on the greater efficiency of the NA of CT and CF in the TZBA than in the UPA.

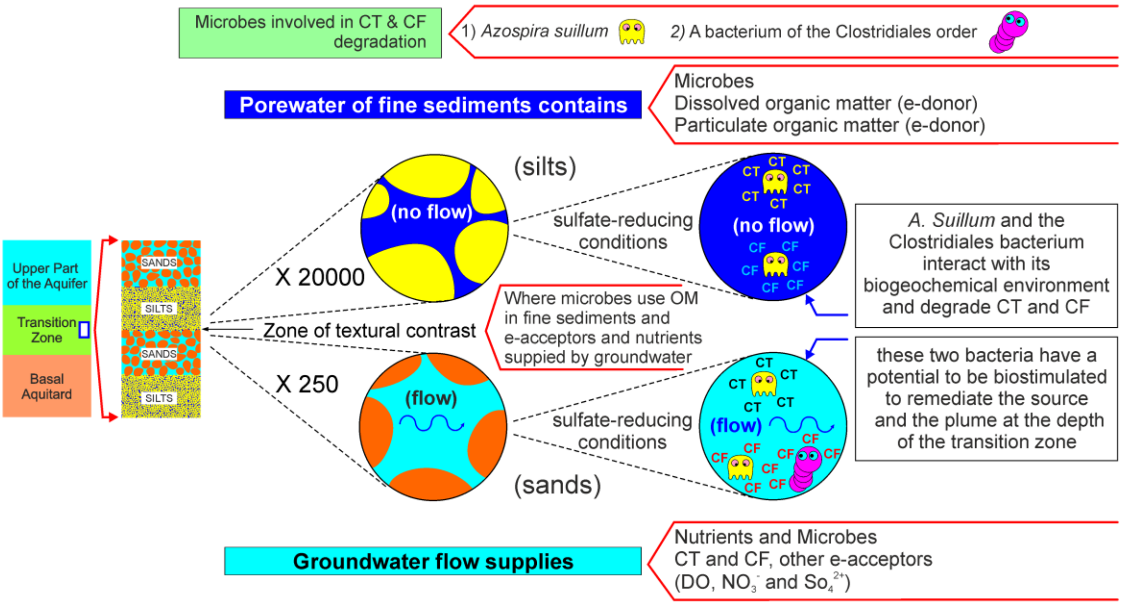

Figure 11. Conceptual model that represents how *A. suillum* and the Clostridiales bacterium interact with the biogeochemical environment.

The high geological heterogeneity in the TZBA, with the presence of numerous interbedded layers of silty-clays, sands, and gravels with variable fine matrix content in this unit (see Section 4.1), accounts for the high textural heterogeneity observed, with abundant textural contrasts between fine and coarse materials. These contrasts result in hydraulic conductivity differences between adjacent layers (Figure 2B), which for the whole TZBA derive in a low hydraulic conductivity and transmissivity (much lower than those in the UPA, see Section 4.1).

According to Goldscheider et al. (2006), contact surfaces between different texture materials become ecotones (a zone where exchanges among two adjacent microbial ecosystems occur, see Section 4.4). Since the TZBA constitutes a succession of numerous texture changes, it can be agreed that this zone as a whole is an ecotone product of the high geological and textural heterogeneity.

Given the low transmissivity in the TZBA, DO supplied to the source and the plume by groundwater flowing through the coarser grain size layers is little (especially at the source, where much of the pores are partially occupied by DNAPL, see Section 4.3.1). In addition to DO, other compounds and elements are provided by groundwater flow: i) more electron acceptors (nitrate, sulfate, CT, CF, and their metabolites), ii) electron donors (such as dissolved organic matter), and iii) nutrients and other components needed by microbes living in groundwater and in the fine grained less-conductive layers, where a large favorable substrate of dissolved and particulate organic matter exists (Naganna, Deka, and Hansen, 2017) acting as carbon and energy sources for microorganisms. The large amount of organic carbon acting as an electron donor causes the small amount of DO that reaches the source and plume to be consumed. This demonstrates the role played by the geological and textural heterogeneity in the development of suitable conditions for the NA of CT and CF, since the consumption of the supplied DO gives rise to a highly anoxic environment (see Sections 4.2.1and 4.3.1) under which the dominant redox conditions become sulfate-reducing (see Sections 4.2.2 and 4.3.2).

These redox conditions, along with components supplied by groundwater and organic matter substrate in the fine material layers, are suitable for *A. suillum* and the bacterium of the order Clostridiales to give rise to the natural reductive dechlorination of CT and CF (and metabolites). They are planktonic microorganisms transported with groundwater (see Section 4.5.1) along the levels of coarse materials in the TZBA. *A. suillum* is small enough to penetrate the finest materials, while the larger cell size of the

Clostridiales bacterium hinders its ability to penetrate those finer materials (see Section 4.5.2). Therefore, geological and textural heterogeneity also control the subsurface distribution of microorganisms that degrade CT and CF.

5. Conclusions

The most important key control exerted on the greater efficiency of natural attenuation of CT and CF in the TZBA than in the UPA is the high geological and textural heterogeneity in the transition zone, resulting from the numerous interbedded silty-clay layers between fine to coarse sands and gravels with variable fine matrix content.

This geological and textural heterogeneity is responsible for the highly anoxic environment under sulfate-reducing dominant redox conditions at the source and the plume. The following factors give rise to the development of conditions suitable for degradation of CT and CF: i) low hydraulic conductivity and transmissivity, which implies a small DO supply with groundwater flow through the coarser grain size layers, and ii) consumption of what little remains of the DO by the high amount of dissolved and particulate organic matter in the finer grain size layers, acting as a carbon and energy source for microorganisms.

As a consequence of the geological and textural heterogeneity, the transition zone constitutes an ecotone, which conditions the diversity and abundance of the microbial ecosystem. Moreover, the pore throat threshold is one of the textural parameters of the of subsurface sediments, and is, therefore, also determined by the geological and textural heterogeneity in the transition zone. This parameter also controls the subsurface distribution of microorganisms, since bacteria size exclusion causes a decrease in the diversity and abundance of microbial communities. Thus, the bacterium of the order Clostridiales, which is a planktonic microorganism that migrates with the groundwater flow and performs the reductive dechlorination of CF to DCM in the coarse and more-conductive materials, is unable to penetrate the finest materials in the transition zone, probably because its cell size is larger than the pore throat threshold value. By contrast, *A. suillum*, which is also a planktonic microorganism involved in the reductive dechlorination of CT and CF in groundwater, is able to enter into the finer and less-conductive materials because its cell size is less than the pore throat threshold. Once inside the PWFS, *A. suillum* accumulates and remains attached to the surface of mineral grains (which accounts for its great abundance in fine materials), where it is implicated in the degradation of the CT and CF that penetrated via molecular diffusion from the more-conductive materials.

Bacteria size exclusion determines, therefore, the penetration of dechlorinating microorganisms into the finest and less-conductive materials and should be an important issue to consider for any contamination scenario in which bioremediation strategies such as biostimulation or bioaugmentation are proposed. These strategies may be ineffective if a significant part of the microorganisms involved cannot enter into the finest contaminated sediments. The relevance of this lies in the need to verify whether the microorganisms involved can physically migrate through the finest sediments before implementing the remediation strategies.

The natural attenuation of CT observed in the transition zone is an abiotic reductive dechlorination process in the presence of green rusts biogenically generated by *A. suillum*. Different evidence indicates the generation of green rusts precipitates as a byproduct of the biogenic activity of *A. suillum* and the role of these Fe-minerals as natural reducing agents of CT to form CF, DCM, and CM (and possibly CH_4) in the transition zone. These proofs indicate that the necessary conditions exist in this zone for *A. suillum* to give rise to green rusts using the Fe(II) content of sediments as electron donors and nitrates as electron acceptors under anoxic conditions: a) the greater abundance of *A. suillum* in the transition zone than in the upper part of the aquifer; b) the dominant sulfate-reducing redox conditions and highly anoxic environment at the transition zone; c) the Fe-reduction of iron oxidized minerals, which delivers Fe^{2+} to the environment; and d) a high denitrification rate and enrichment factor for ^{15}N. This evidence also shows that the formation of green rusts in the transition zone is also a consequence of the intrinsically high geological and textural heterogeneity in this hydrostratigraphic unit.

Given the favorable conditions for natural attenuation of CT and CF in the transition zone, *A. suillum* and the Clostridiales bacterium have a potential to be biostimulated to promote the remediation of CT and CF in the source and the plume in this hydrostratigraphic unit.

Two important questions are derived from the present study that should be answered when designing aquifer biostimulation or bioaugmentation schemes: (1) Which indigenous microorganisms are involved in the natural attenuation of contaminants? (2) Under which dominant redox conditions are these microorganisms more efficient? (3) In the case of fine materials into which pollutants penetrate by molecular diffusion, is the size of their cells greater than the threshold value? In this case, it would be possible to combine biostimulation and bioaugmentation schemes to avoid the rebound effect. This information is of particular relevance in cases in which a DNAPL source in the aquifer is in a transition zone (given the longevity of the sources in these cases). These factors have important environmental implications for two reasons: (1) many supply wells exploit aquifers in basins in which land uses are devoted to industries related to the frequent use or handling of chlorinated solvents and (2) from the geological point of view, these basins are frequently filled with clastic sediments that constitute alluvial fan deposits and sheet floods that correspond to transition zones with numerous fine-grained layers above which DNAPL pools accumulate.

Acknowledgments

We are indebted to the Catalan Water Agency and members of the company Clariant Ibérica S.A. of Tarragona for the support and cooperation while carrying out the field work. We would also like to thank the members of the Scientific and Technological Centers of the University of Barcelona. At the same time, we would like to acknowledge the institutions that financed the research within the following research projects: CTM 2005–07824 and CGL 2008-02164/BTE funded by the Spanish Ministry of Education and Science and Clariant Ibérica S.A.

References

Achenbach, L.A.; Michaelidou, U.; Bruce, R.A.; Fryman, J. and Coates, J.D. (2001). *Dechloromonas agitata* gen. nov., sp. nov. and *Dechlorosoma suillum* gen. nov., sp. nov., two novel environmentally dominant (per)chlorate-reducing bacteria and their phylogenetic position. International Journal of Systematic and Evolutionary Microbiology, 51:527–533. http://dx.doi:10.1099/00207713-51-2-527

Alexander, M. (1978). Introduction to soil microbiology. Soil Science, 125(5):331.

Alvarez, L.H.; Jimenez-Bermudez, L.; Hernandez-Montoya, V. and Cervantes, F.J. (2012). Enhanced dechlorination of carbon tetrachloride by immobilized fulvic acids on alumina particles. Water, Air, and Soil Pollution, 223(4):1911–1920.

Amodu, O.S.; Ojumu; T.V. and Ntwampel , S.K.O. (2013). Bioavailability of high molecular weight polycyclic aromatic hydrocarbons using renewable resources. In Environmental Biotechnology-New Approaches and Prospective Applications. Intech (chapter 8). Environmental Biotechnology - New Approaches and Prospective Applications. http://dx.doi.org/10.5772/54727.

Assaf-Anid, N. and Lin, K.Y. (2002). Carbon tetrachloride reduction by Fe^{2+}, S^{2-}, and FeS with vitamin B_{12} as organic amendment. Journal of environmental engineering, 128(1):94–99.

Bouwer, E.J. (1994). Bioremediation of chlorinated solvents using alternate electron acceptors. In: Matthews, J.E. (Ed.), Handbook of Bioremediation. Lewis Publishers, London, pp. 149–175.

Chan, C.C.; Mundle, S.O.; T. Eckert, X. Liang, S. Tang, G. Lacrampe-Couloume, E.A. Edwards and B. Sherwood Lollar (2012). Large carbon isotope fractionation during biodegradation of chloroform by *Dehalobacter* cultures. Environmental science & technology. 46:10154–10160.

Chaudhuri, S.K.; Lack, J.G. and Coates, J.D. (2001). Biogenic Magnetite Formation through Anaerobic Biooxidation of Fe (II). Applied and Environmental Microbiology, 67(6):2844–2848. doi: 10.1128/AEM.67.6.2844-2848.

Christensen, T.H.; Bjerg, P.L.; Banwart, S.A.; Jakobsen, R.; Heron, G. and Albrechtsen, H.J. (2000). Characterization of redox conditions in groundwater contaminant plumes. Journal of Contaminant Hydrology, 45(3-4):165-241.

Cohen, R.M. and Mercer, J.W. (1993). DNAPL Site Investigation. C.K. Smoley, Boca Raton, USA.

Cycoń, M.; Markowicz, A.; Borymski, S.; Wójcik, M. and Piotrowska-Seget, Z. (2013). Imidacloprid induces changes in the structure, genetic diversity and catabolic activity of soil microbial communities. Journal of environmental management, 131:55-65.

Da Lima, G.P. and Sleep, B.E. (2010). The impact of carbon tetrachloride on an anaerobic methanol-degrading microbial community. Water, Air, and Soil Pollution, 212(1-4):357-368.

Davis, A.; Fennemore, G.G; Peck, C.; Walker, C.R.; McIlwraith, J. and Thomas, S. (2003). Degradation of carbon tetrachloride in a reducing groundwater environment: Implications for natural attenuation. Applied Geochemistry, 18:503–525.

Dogramaci, S.S.; Herczeg, A.L.; Schiff, S.L.; Bone, Y. (2001). Controls on $\delta^{34}S$ and $\delta^{18}O$ of dissolved SO_4 in aquifers of the Murray Basin, Australia and their use as indicators of flow processes. Applied Geochemistry, 16:475–488.

Einarson, M., Fure, A., St. Germain, R., Chapman, S. and Parker, B. (2018). DyeLIF™: A New Direct-Push Laser-Induced Fluorescence Sensor System for Chlorinated Solvent DNAPL and Other Non-Naturally Fluorescing NAPLs. Groundwater Monitoring & Remediation, 38(3):28-42.

Farthing, M.W.; Seyedabbasi, M.A.; Imhoff, P.T. and Miller, C.T. (2012). Influence of porous media heterogeneity on nonaqueous phase liquid dissolution fingering and upscaled mass transfer. Water Resources Research, 48(W08507). doi:10.1029/2011WR011389.

Fetter, C.W.; Boving, T.; and Kreamer, D. (2017). Contaminant hydrogeology. Waveland Press.

Fjordbøge, A.S.; Janniche, G.S.; Jørgensen, T.H.; Grosen, B.; Wealthall, G.; Christensen, A.G.; Kerrn-Jespersen, H. and Broholm, M. M. (2017). Integrity of clay till aquitards to DNAPL migration: Assessment using current and emerging characterization tools. Groundwater Monitoring & Remediation, 37(3):45-61.

Fraser, P.J.; Dunse, B.L.; Manning, A.J.; Walsh, S.; Wang, R.H.J.; Krummel, P.B. and Simmonds, P.G. (2014). Australian carbon tetrachloride emissions in a global context. Environmental Chemistry, 11(1):77-88.

Fukada, T.; Hiscock, K.M.; Dennis, P.F.; Grischek, T. (2003). A dual isotope approach to identify denitrification in groundwater at a river bank infiltration site. Water Research, 37:3070–3078

Goldscheider, N.; Hunkeler, D. and Rossi, P. (2006). Review: microbial biocenoses in pristine aquifers and an assessment of investigative methods. Hydrogeology Journal, 14(6):926–941.

Grostern, A.; Duhamel, M.; Dworatzek, S. and Edwards, E.A. (2010). Chloroform respiration to dichloromethane by a *Dehalobacter* population. Environmental microbiology, 12(4):1053-1060.

Hartog H.; Cho J.; Parker B.L.; Annable, M.D. (2010) Characterization of a heterogeneous DNAPL source zone in the Borden aquifer using partitioning and interfacial tracers: residual morphologies and background sorption. J Contam Hydrol 115(1):79–89.

Herrmann, M., Wegner, C. E., Taubert, M., Geesink, P., Lehmann, K., Yan, L. Lehmann, R. and Küsel, K. (2019). Predominance of Cand. Patescibacteria in groundwater is caused by their preferential mobilization from soils and flourishing under oligotrophic conditions. Frontiers in Microbiology, 10, 1407.

Hunkeler, D., Meckenstock, R.U., Sherwood Lollar, B., Schmidt, T.C., Wilson, J.T., Schmidt, T. and Wilson, J. (2008). A guide for assessing biodegradation and source identification of organic ground water contaminants using compound specific isotope analysis (CSIA). Oklahoma, USA, US EPA.

Hunkeler, D.; Abe, Y.; Broholm, M.M.; Jeannottat, S.; Westergaard, C.; Jacobsen, C.S. and Bjerg, P.L. (2011). Assessing chlorinated ethene degradation in a large scale contaminant plume by dual carbon–chlorine isotope analysis and quantitative PCR. Journal of contaminant hydrology, 119(1):69–79.

Imhoff, P.T.; Jaffe, P.R. and Pinder G.F. (1994), An experimental study of complete dissolution of a nonaqueous phase liquid in saturated porous media. Water Resources Research, 30(2):307–320. https://doi.org/10.1029/93WR02675.

ITRC (Interstate Technology & Regulatory Council). (2015). Integrated DNAPL Site Characterization and Tools Selection (ISC-1).

Joergensen, R.G. and Wichern, F. (2018). Alive and kicking: Why dormant soil microorganisms matter. Soil Biology and Biochemistry, 116:419-430.

Johnston, D. (2006). Draft EPA Guidelines Regulatory Monitoring and Testing Groundwater Sampling 56. Environment Protection authority (EPA), Australia.

Justicia-Leon, S.D.; Higgins, S.; Mack, E.E.; Griffiths, D.R.; Tang, S.; Edwards, E.A. and Löffler, F.E. (2014). Bioaugmentation with distinct *Dehalobacter* strains achieves chloroform detoxification in microcosms. Environmental science & technology, 48(3):1851-1858.

Lack, J.G.; Chaudhuri, S.K.; Chakraborty, R.; Achenbach, L.A. and Coates, J.D. (2002). Anaerobic biooxidation of Fe (II) by *Dechlorosoma suillum*. Microbial ecology, 43(4):424-431.

Liang, X. and Butler, E.C. (2010). Effects of natural organic matter model compounds on the transformation of carbon tetrachloride by chloride green rust. Water Research, 44(7):2125-2132.

Luciano, A.; Viotti, P. and Papini, M.P. (2010). Laboratory investigation of DNAPL migration in porous media. Journal of Hazardous Materials, 176(1):1006-1017.

Mackay, D.M. and Cherry, J.A. (1989). Groundwater contamination: pump-and treat remediation. Environmental Science and Technology 23, 630–636.

Matocha, C.J.; Dhakal, P. and Pyzola, S.M. (2012). The role of abiotic and coupled biotic/abiotic mineral controlled redox processes in nitrate reduction. In Advances in agronomy (Vol. 115, pp. 181-214). Academic Press.

Muyzer, G.; De Waal, E.C. and Uitterlinden, A.G. (1993). Profiling of complex microbial populations by denaturing gradient gel electrophoresis analysis of polymerase chain reaction-amplified genes coding for 16S rRNA. Applied and Environmental Microbiology, 59(3):695-700.

Naganna, S. R., Deka, P. C., Ch, S. and Hansen, W. F. (2017). Factors influencing streambed hydraulic conductivity and their implications on stream–aquifer interaction: a conceptual review. Environmental Science and Pollution Research, 24(32), 24765-24789.

Nam, J.H.; Ventura, J.R.S.; Yeom, I.T.; Lee, Y. and Jahng, D. (2016). A novel perchlorate-and nitrate-reducing bacterium, *Azospira*. Applied microbiology and biotechnology, 100(13):6055-6068.

O'Loughlin, E.J.; Kemner, K.M. and Burris, D.R. (2003). Effects of Ag, Au and Cu on the reductive dechlorination of carbon tetrachloride by green rust. Environmental Science & Technology. 37:2905–2912.

Palau, J.; Soler, A.; Teixidor, P. and Aravena, R. (2007). Compound-specific carbon isotope analysis of volatile organic compounds in water using solid-phase microextraction. Journal of Chromatography A, 1163:260–268.

Pankow, J.F.; Cherry, J.A. (1996). Dense Chlorinated Solvents and other DNAPL's in Groundwater: History, Behavior, and Remediation. Waterloo Press, Portland, Oreg. U.S.A.

Parker, B.L.; Chapman, S.W.; and Guilbeault, M.A. (2008). Plume persistence caused by back diffusion from thin clay layers in a sand aquifer following TCE source-zone hydraulic isolation. Journal of Contaminant Hydrology, 102:86–104.

Parker, B.L.; Cherry, J.A. and Chapman, S.W. (2004). Field study of TCE diffusion profiles below DNAPL to assess aquitard integrity. Journal of Contaminant Hydrology, 74(1):197-230.

Parker, B.L.; Cherry, J.A.; Chapman, S.W. and Guilbeault, M.A. (2003). Review and analysis of chlorinated solvent dense nonaqueous phase liquid distributions in five sandy aquifers. Vadose Zone Journal, 2:116–137.

Penny, C.; Gruffaz, C.; Nadalig, T.; Cauchie, H.M.; Vuilleumier, S. and Bringel, F. (2015). Tetrachloromethane-degrading bacterial enrichment cultures and isolates from a contaminated aquifer. Microorganisms, 3(3):327-343.

Penny, C.; Vuilleumier, S. and Bringel, F. (2010). Microbial degradation of tetrachloromethane: mechanisms and perspectives for bioremediation. FEMS microbiology ecology, 74(2):257-275.

Portillo, M. C., Leff, J. W., Lauber, C. L. and Fierer, N. (2013). Cell size distributions of soil bacterial and archaeal taxa. Applied and environmental microbiology, AEM-02710.

Puigserver, D.; Carmona, J.M.; Cortés, A.; Viladevall, M.; Nieto, J.M.; Grifoll, M. and Parker, B.L. (2013). Subsoil heterogeneities controlling porewater contaminant mass and microbial diversity at a site with a complex pollution history. Journal of contaminant hydrology, 144(1):1-19.

Puigserver, D.; Cortés, A.; Viladevall, M.; Nogueras, X.; Parker, B.L. and Carmona, J.M. (2014). Processes controlling the fate of chloroethenes emanating from DNAPL aged sources in river–aquifer contexts. Journal of contaminant hydrology, 168:25-40.

Puigserver, D.; Herrero, J.; Torres, M.; Cortés, A.; Nijenhuis, I.; Kuntze, K. and Carmona, J.M. (2016a). Reductive dechlorination in recalcitrant sources of chloroethenes in the transition zone between aquifers and aquitards. Environmental Science & Pollution Research, 23(18):18724-18741.

Puigserver, D.; Herrero, J.; Torres, M.; Cortés, A.; Nijenhuis, I.; Kuntze, K. and Carmona, J.M. (2016b). Degradation of chloroethenes in the transition zone between aquifers and aquitards. WIT Transactions on Ecology and the Environment. 209:115-126.

Puigserver, D.; Nieto, J.M.; Grifoll, M.; Vila, J.; Cortés, A.; Viladevall, M. and Carmona, J.M. (2016c). Temporal hydrochemical and microbial variations in microcosm experiments from sites contaminated with chloromethanes under biostimulation with lactic acid. Bioremediation Journal. 20(1):54-70.

Puls, R.W.; Barcelona, M.J. (1996). Low-flow (minimal drawdown) ground-water sampling procedures. Ground Water Issue 12. EPA.

Ramsburg, C.A.; Thornton, C.E. and Christ, J.A. (2010). Degradation product partitioning in source zones containing chlorinated ethene dense non-aqueous-phase liquid. Environmental science & technology, 44(23):9105-9111.

Rivett, M. O., Dearden, R. A. and Wealthall, G. P. (2014). Architecture, persistence and dissolution of a 20 to 45 year old trichloroethene DNAPL source zone. Journal of contaminant hydrology, 170:95-115.

Rotiroti, M.; Jakobsen, R.; Fumagalli, L. and Bonomi, T. (2018). Considering a threshold energy in reactive transport modeling of microbially mediated redox reactions in an arsenic-affected aquifer. Water, 10(1):90.

Shuangfang, L.U., Junqian, L.I., ZHANG, P., Haitao, X U.E., Guoli, W.A.N.G., ZHANG, J. and Zheng, L.I. (2018). Classification of microscopic pore-throats and the grading evaluation on shale oil reservoirs. Petroleum Exploration and Development, 45(3):452-460.

Silva, S.R.; Kendall, C.; Wilkinson, D.H.; Ziegler, A.C.; Chang, C.C.Y.; Avanzino, R.J. (2000). A new method for collection of nitrate from fresh water and the analysis of nitrogen and oxygen isotope ratios. Journal of Hydrology, 228:22–36.

Trevors, J.T. (1996). Sterilization and inhibition of microbial activity in soil. Journal of Microbiological Methods, 26:53–59.

US Environmental Protection Agency (2008). A guide for assessing biodegradation and source identification of organic ground water contaminants using compound specific isotope analysis (CSIA). Ada, OK: Office of Research and Development, US Environmental Protection Agency.

Vickstrom, K.E.; Azizian, M.F. and Semprini, L. (2017). Transformation of carbon tetrachloride and chloroform by trichloroethene respiring anaerobic mixed cultures and supernatant. Chemosphere, 182:65-75.

Vikesland, P.J.; Heathcock, A.M.; Rebodos, R.L. and Makus, K.E. (2007). Particle size and aggregation effects on magnetite reactivity toward carbon tetrachloride. Environmental science & technology, 41(15):5277-5283.

Wanner, P.; Parker, B.L.; Chapman, S.W.; Aravena, R. and Hunkeler, D. (2016). Quantification of Degradation of Chlorinated Hydrocarbons in Saturated Low

Permeability Sediments Using Compound-Specific Isotope Analysis. Environmental science & technology, 50(11):5622-5630.

Weatherill, J. J.; Atashgahi, S.; Schneidewind, U.; Krause, S.; Ullah, S.; Cassidy, N.; and Rivett, M.O. (2018). Natural attenuation of chlorinated ethenes in hyporheic zones: a review of key biogeochemical processes and in-situ transformation potential. Water research, 128:362-382.

Weber, K.A.; Achenbach, L.A. and Coates, J.D. (2006). Microorganisms pumping iron: anaerobic microbial iron oxidation and reduction. Nature Reviews Microbiology, 4(10):752-764.

Xiao, X.; Prinn, R.G.; Fraser, P.J.; Weiss, R.F.; Simmonds, P.G.; O'Doherty, S. and Golombek, A. (2010). Atmospheric three-dimensional inverse modeling of regional industrial emissions and global oceanic uptake of carbon tetrachloride. Atmospheric Chemistry and Physics, 10(21):10421-10434.

Yin, W., Strobel, B.W. and B. Hansen, H.C. (2017). Amino Acid-Assisted Dehalogenation of Carbon Tetrachloride by Green Rust: Inhibition of Chloroform Production. Environmental Science & Technology, 51(6):3445-3452.